



Cite this: *Green Chem.*, 2021, **23**, 8305

## Progress in marine derived renewable functional materials and biochar for sustainable water purification

Halanur M. Manohara, <sup>a</sup> Sooraj S. Nayak, <sup>a</sup> Gregory Franklin, <sup>b</sup> Sanna Kotrappanavar Nataraj <sup>\*a,c</sup> and Dibyendu Mondal <sup>\*a,b</sup>

Global water scarcity is increasing day-by-day due to population explosion, urbanization and rapid industrialization. Inevitably, surface water is widely contaminated by various hazardous geogenic, organic and inorganic contaminants, also by untreated industrial effluents and unscientific human activities. On the other hand, the rapid worldwide increase in consumption of petroleum products has inspired researchers to develop renewable and sustainable materials for water purification applications. Significantly, biomass-derived materials are promising substitutes for depleting resources. Specifically, marine-based biomaterials, for instance, chitin/chitosan, seaweeds and seaweed-based polysaccharides (agarose, alginate, cellulose, carrageenan) are abundant, environmentally friendly, and renewable biomaterials that are considered an appropriate solution for environmental contamination. Over past few decades various studies have focused on marine-based and seaweed-polysaccharide-based composites because of their renewability and sustainability for water purification. A number of reviews exist for biopolymer-based material applications in water purification; but to promote marine-derived biomaterials for water purification, a critical review between conventional materials and emerging approaches using seaweed-derived materials is needed. Hence, the present review study is the first of its kind, shedding light on the selection of diverse marine-derived biomaterials, as well as their important physical and chemical properties, in order to design functional materials for water purification applications. Further, the present review critically assesses the high-performance marine-derived functional materials exploited for existing state-of-the-art water purification technologies. Marine-derived materials with unique properties, such as inbuilt functionality, high mechanical strength, and prominent surface area and their prominence in developing high-performance sustainable materials for water purifications are reviewed. Furthermore, the review also discusses the various methodologies developed for the preparation of multifunctional carbonaceous materials using marine-derived biomaterials. Such biochar compete with commercial activated carbon and graphene owing to their unique properties. Also, the challenges in implementing the developed functional biomaterials in state-of-the-art water purification technologies and future prospects are discussed.

Received 23rd August 2021,  
Accepted 6th October 2021

DOI: 10.1039/d1gc03054j  
[rsc.li/greenchem](http://rsc.li/greenchem)

### 1. Introduction

Over the past few decades, biomass valorisation as a green renewable resource has received a lot of attention globally from research sectors and industries.<sup>1-3</sup> With the rapid deterioration in renewable fossil fuel resources and growing environmental problems, many researchers are attempting to produce biofuels,<sup>4</sup> value-added chemicals,<sup>5</sup> carbonaceous

materials<sup>6</sup> as well as functional composites for various applications.<sup>7,8</sup> With diminishing resources for synthetic polymers, such as petroleum and non-renewable carbon sources, there has been growing interest in biomass-derived macromolecules because of their unique characteristics and because they are potential substitutes for synthetic polymers.<sup>9,10</sup> Importantly, they are abundant, biodegradable, economic, non-toxic and also it is easy to manipulate their physico-chemical properties for desired applications. About 70% of the Earth's surface is covered by ocean which represents a vast resource of biodiversity. Moreover, marine organisms have adapted to extreme environments, such as high salinity, pH, high pressure and temperature and, hence, their biochemical composition provides an exceptional reservoir to explore and design functional materials.<sup>11,12</sup> Seaweed-based materials

<sup>a</sup>Centre for Nano and Material Sciences, JAIN University, Jain Global Campus, Bangalore 562112, India. E-mail: [sk.nataraj@jainuniversity.ac.in](mailto:sk.nataraj@jainuniversity.ac.in), [dmtapu@gmail.com](mailto:dmtapu@gmail.com), [m.dibyendu@jainuniversity.ac.in](mailto:m.dibyendu@jainuniversity.ac.in)

<sup>b</sup>Institute of Plant Genetics of the Polish Academy of Sciences, 60-479 Poznan, Poland

<sup>c</sup>IMDEA Water Institute, Avenida Punto Com, 2. Parque Científico Tecnológico de la Universidad de Alcalá, Alcalá de Henares 28805 Madrid, Spain

from the oceans, produced in copious quantities of over 19 million tonnes and either harvested from the oceans or cultured annually, are promising feedstocks for the production of sustainable functional materials.<sup>13,14</sup> Seaweeds are found throughout the world's oceans and are mainly classified as brown seaweed (Phaeophyta) and red seaweed (Rhodophyta), which are exclusively marine, and green seaweed (Chlorophyta) which are freshwater and terrestrial, based on their colour appearance.<sup>15,16</sup> Seaweed contains a huge amount of bioactive components, such as pigments, phenols, proteins, polysaccharides, and bioactive peptides. A vast amount of research has explored marine-derived biomaterials as food sources and their health benefits have been demonstrated. Further, various value-added chemicals, biopolymers, carbohydrates and macromolecules have been successfully extracted and employed for various applications, such as biofuel production,<sup>17</sup> catalysis,<sup>18,19</sup> energy storage and conversion,<sup>20–22</sup> biological applications and environmental applications (Fig. 1).<sup>23</sup> Consequently, there is an increase in attention towards developing a marine bioprocess industry to valorise biomaterials into valuable functional materials through facile chemical processes.

On the other hand, with the increase in global water scarcity, the supply of affordable potable water is a massively challenging proposition throughout the world. Rapid industrialization and rising environmental contamination of natural water sources need to be tackled on a priority basis. Unfortunately, current water purification technologies are noneconomic and inefficient for meeting existing demands.<sup>24,25</sup> Besides this, most existing materials are non-biodegradable and difficult to recycle, and disposal of these materials can cause secondary pollution that has led to rising concerns by occupational and environmental health experts that they are more harmful materials than previously encountered ones in causing serious threat to life forms.<sup>3,26</sup> Therefore, there is a growing concern to develop low-cost, sustainable efficient functional materials

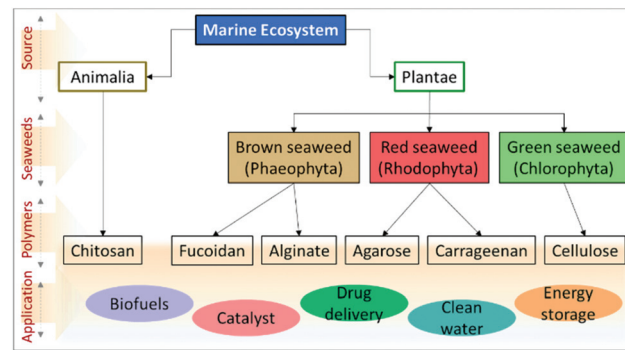
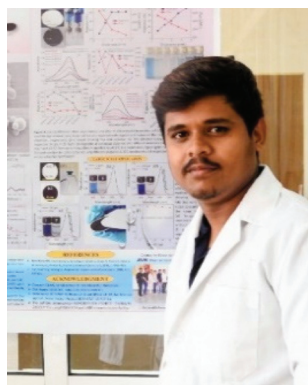


Fig. 1 Flow chart representing the types of marine-derived biomaterials and extracted biomacromolecules.

using biopolymers or polymeric organic molecules acquired from renewable resources.<sup>26–28</sup> Apart from cellulose from terrestrial plant-based materials, seaweed-derived macromolecules are the most exploited materials in water purification technologies thanks to their remarkable mechanical strength, enriched functionalities, moderate surface area and chemical stability. Generally, polysaccharide derivatives showed high removal efficiency for various organic contaminants (e.g. dyes, drugs, pesticides) and inorganic contaminants (fluoride, phosphates, heavy metal ions) *via* biosorption, adsorption, coagulation, reduction and oxidation.<sup>29,30</sup> In particular, seaweed-based biomaterials possess extensive hydroxyl and amine functionalities and exhibit considerably high metal binding capacity and selectivity attributed to metal-ligand interaction, which creates the opportunity to develop efficient functional materials for water purification technologies.<sup>31</sup> However, inevitably seaweed-derived materials need to be reformed through chemical or physical surface modifications in order to remove these organic compounds, since they dissolve in water with varying pH values.



Halunur M. Manohara

aerogels and composite membranes for wastewater treatment. He also obtained the AWSAR Award-2020 in a contest organized by the Department of Science and Technology, India for his best research story.



Sooraj S. Nayak

Mr Sooraj worked as a Project Assistant at CNMS, Jain University, Bangalore, Karnataka, India. He completed an MSc in chemistry in 2020 from Alva's college, Karnataka, India. Since childhood, he was fascinated by science and accordingly chose a career in chemistry.

He also believes that material science has true potential to revolutionize the way of living in synergy with nature to make the world a better place. Mr Sooraj

is looking forward to working in fields such as water treatment, nanotechnology and biomaterials.

Hence, over the past few decades various research groups have extensively developed derivatives of seaweed-based biomaterials by simple complexation with polymers, biopolymers, and nanocomposites. Further, they have also utilised them as a low-cost feedstock to prepare valuable carbonaceous materials with high surface area, surface functionality, and heteroatom and metal doped carbonaceous materials by following simple high-temperature treatment.<sup>32</sup> Thus, the present review sheds light on various seaweed-derived macromolecules used to engineer and develop high-performance seaweed-based materials, their physico-chemical properties and potential application in water purification technologies. Further, this review will encourage material scientists to fully utilise the hidden potential of marine-derived biomaterials in the field of sustainable water purification.

## 2. Raw seaweed-based materials

Generally seaweed-based materials containing a huge amount of organic polymers made up of carbohydrates and proteins are produced globally on a large scale from red, green and brown seaweeds.<sup>33</sup> Understanding their structure and diversity in chemical composition can help us gain insight into material design and can also inspire the development of high-performance materials.

Although, seaweeds have significant importance in food and industrial applications, in the late 20<sup>th</sup> century, extensive research was done utilising marine-derived materials such as seaweeds and polysaccharides for ion exchange, adsorption or biosorption applications after suitable chemical pre-treatment (Fig. 2).<sup>34</sup> The biosorption capability of seaweeds is related to the chemical composition of the cell walls. Seaweed generally contains extensive amounts of hydroxyl, acetamide, amine,

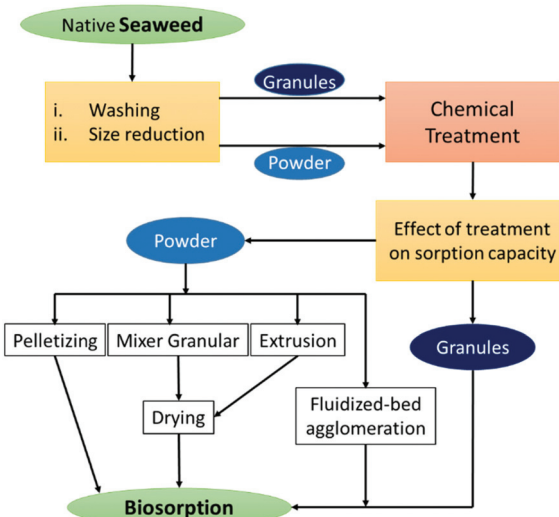


Fig. 2 General schematic representation of the preparation of biosorbents from seaweeds.

amide, sulfate and phosphate functional groups, significantly enabling metal-ligand interaction, which helps in capturing heavy metal ions from an aqueous medium.<sup>35–37</sup> In particular, alginate is more responsible for the biosorption in brown algae, carragenan in red seaweed and agarose in green seaweed.<sup>38</sup> Various seaweeds exhibit notable biosorption capacity for heavy metal ions and are listed in Table 1. In 1987, Volesky and Kuyucak established the biosorption of silver ions from waste industrial effluents using *Sargassum* seaweed and patented the same.<sup>39</sup> Several interaction mechanisms, such as coordination, chelation, electrostatic interaction, complexation, ion-exchange and physical adsorption have been anticipated for the separation of heavy metal ions. Lately, *Sargassum*



Gregory Franklin

green chemistry and the interaction between plants and nano-materials is the main focus of his research team.



Sanna Kotrappanavar  
Nataraj

Dr S. K. Nataraj is currently working as a Professor at CNMS, Jain University, Bangalore, India. He obtained his PhD in 2008 in Polymer Science from Karnataka University, Dharwad, India. Immediately after the completion of his PhD, he pursued three Postdoctoral Associate assignments at Chonnam National University, South Korea (2007–2009), Institute of Atomic Molecular Sciences, Academia Sinica (2009–10), Taiwan and the Cavendish Laboratory, University Cambridge, UK (2010–2013). He was awarded the DST-INSPIRE Faculty Award (2013–2015) at CSIR-CSMCRI, Bhavnagar. His main areas are the development of sustainable materials and processes for Energy and Environmental applications including water treatment.

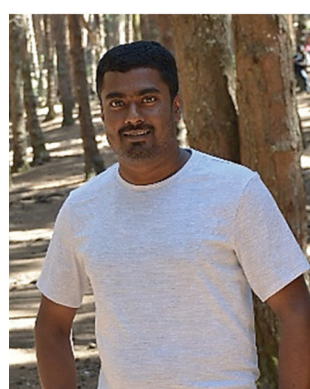
**Table 1** Seaweed and seaweed-derived high-performance carbonaceous materials explored for water purification applications

Sl. no.	Seaweed-based biomass	Modifying agent	Pollutants	Ads. ( g)	Ref.
01	<i>Sargassum</i> sp.	—	Pb	1.1 mmol	40
02	<i>Sargassum</i> sp.		Cu	0.9 mmol	
03	<i>Padina</i> spp.	—	Cd	0.7 mmol	41
04	<i>Gracilaria</i> spp.		Pb	1.2 mmol	40
05	<i>Sargassum vulgare</i>	—	Cu	1.1 mmol	
06	<i>Fucus vesiculosus</i>		Pb	0.4 mmol	40
07	<i>Ascophyllum nodosum</i>	NaOH treatment	Cu	0.5 mmol	
08	<i>Ulva</i> spp.	Alkali treatment	Cd	87 mg	40
			Cu	59 mg	
09	<i>Durvillaea potatorum</i>	CaCl <sub>2</sub> solution treatment	Cr III	74.6 mg	
10	<i>Ecklonia radiata</i>	CaCl <sub>2</sub> solution treatment	Cr VI	1.2 mmol	42
11	<i>Durvillaea potatorum</i>	CaCl <sub>2</sub> solution treatment	Co	0.8 mmol	
12	<i>Sargassum filipendula</i>	Dealginated, acid treatment	Cd	160 mg	43
13	<i>Sargassum fluitans</i>	Acid wash, protonated	Zn	90.7 mg	
14	<i>Enteromorpha torta</i>	Immobilised in alginate	Ni II	74.6 mg	44
15	Seaweed community biomass	Alkali treatment	Cd II	57.3 mg	
16	Red seaweed	Citric acid	Pb	1.1 mmol	45
17	<i>Stoechospermum marginatum</i>	(i) Propylamine, (ii) methanol, (iii) formaldehyde, (iv) formic acid	Cu	1.3 mmol	46
			Pb	1.6 mmol	
			Cu	1.3 mmol	47
			Pb	1.3 mmol	
			Cu	1.1 mmol	
			Cu	3.5 mmol	48
			U VI	560 mg	49
			<sup>134</sup> Ce	12.6 mmol	50
			Zn II	115.1 mg	51
			Crystal violet	217.3 mg	52
			Acid orange II	(i) 71 mg, (ii) 29 mg, (iii) 34 mg, (iv) 15 mg	53

has also been explored for the adsorption of lead, copper and cadmium ions with notable biosorption capacity attributed to several advantages, such as high efficiency and affinity for toxic metals, ease of operation, minimisation of the volume of chemical and biological sludge to be disposed of, and low operating cost.<sup>40,41</sup>

Further, researchers have demonstrated that *Durvillaea potatorum* and *Ecklonia radiata* display higher biosorption

capacity for nickel, copper and lead ions compared to *Sargassum*.<sup>45,47,54</sup> In fact, biosorption occurs in two stages: (i) rapid ion-exchange with surface functionalities, and (ii) slow biosorption into the multi-structured material. It is important to note that seaweed-based materials are capable of adsorbing only cationic pollutants. The anionic surface charge of the seaweeds repels anionic pollutants and exhibits poor biosorption. Researchers have also demonstrated chemical activation, such as an acid/alkali wash to activate surface functionalities and enhance the biosorption, with further soaking in calcium, magnesium and potassium salts to prevent the leaching of alginate.<sup>43,47</sup> However, dealginated biomass waste was also explored for biosorption where remarkable efficiency was obtained for the separation of copper ions.<sup>48</sup> This may be due to the voids created after alginic extraction. Interestingly, seaweed-immobilised alginic beads showed superior biosorption for radioactive cesium.<sup>50</sup> Similarly, agar-extracted *Gelidium sesquipedale* exhibited a considerable amount of Cd (ii) biosorption, and equilibrium and kinetic behaviour were further studied to promote the scaling-up process.<sup>55</sup> Furthermore, waste seaweed also showed excellent separation of Pb/Cu and Pb/Cd in a fixed-bed column through a robust ion-exchange process.<sup>56</sup> Similarly, research efforts were made to functionalize seaweed biomaterials for dye biosorption, but the adsorption capacity was comparatively low.<sup>52,53,57</sup> Interestingly, seaweeds were also utilised to prepare biogenic TiO<sub>2</sub> and silver nanoparticles which exhibit photocatalytic activity for the degradation of organic pollutants.<sup>31,58</sup> On the other hand, the contamination of natural habitats with micro-

**Dibyendu Mondal**

Dr Dibyendu Mondal is an ERA chair holder in the NANOPLANT project at IPG PAS, Poznan, Poland from September 2021. He received a PhD in Chemical Science from CSIR-CSMCRI, India in 2015. From 2015 to 2017 he was a postdoc at CICECO, University of Aveiro, Portugal and then he joined CNMS, Jain University, India as an assistant professor in 2017. His main research areas focus on value addition of bio resources

within the biorefinery concept; green solvents mediated the packing of biomolecules. He is also fascinated by designing green nanocomposites for task-specific applications, such as biocatalysis, water purification, and in plant science.

plastics is an emerging concern. Thus, a lot of research has been conducted to develop bio-based plastic using non-renewable resources.<sup>59</sup> Remarkably, in a recent flurry of research, seaweed residue was utilised to develop biodegradable plastics.<sup>60</sup> Interestingly, the inorganic salts present in the micro-algae act as a filler and crosslinker which enhances the practical feasibility of the bioplastic. This finding opens up a new research arena of utilising seaweed residues for the preparation of bioplastics. Despite substantial progress in understanding seaweed-based materials for biosorption and other applications over decades of unceasing research, seaweed-assisted biosorption is still limited to the bench scale. This is due to the poor recyclability, comparatively low biosorption capacity, challenging desorption processes and risk of macromolecules and nanocomposites leaching into the reaction medium during biosorption.<sup>61,62</sup> Also, feasible seaweed-assisted biosorption demands a crucially engineered and developed reactor system and a critical understanding of the processes. With the above-mentioned limitations on seaweed-based biosorption, extensive efforts were made to design and develop functionalised seaweed-derived macromolecules and marine-based discrete biomaterials for various applications. With an extracted distinct macro-molecule with familiar physico-chemical properties, one can tune the adsorption-desorption processes and control the leaching of composites. Over past decades, marine-derived bio-macromolecules, such as alginates, chitin/chitosan, agar/agarose, carrageenan, cellulose, collagen, and fucoidan (Fig. 3) have been developed as highly efficient functional materials for the purification of contaminated groundwater, industrial and domestic wastewater, and also in desalination processes. Fig. 4 shows the number of studies reported from 1995 until now, which indicate a massive growth in marine-derived materials for adsorption,

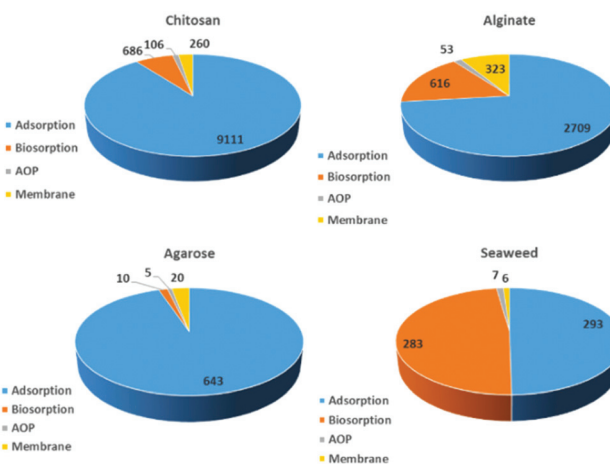


**Fig. 4** Approximate distribution of publications dealing with majorly used marine-derived biopolymers for adsorption, biosorption, advanced oxidation processes (AOP) and membrane filtration according to the Web of Science from 1995 to July 2021.

biosorption, membrane filtration and advanced oxidation processes. Accordingly, we first discuss the structure–property relationship of chitosan and various seaweed-derived biopolymers and then summarize the different approaches developed to prepare high-performance hybrid materials.

### 3. Chitin/chitosan

Chitin/chitosan are the most abundant, renewable, marine-based, N-containing polysaccharides found in the exoskeletons of crustaceans, crabs, insects, algae, fungi and shrimp shells.<sup>63,64</sup> Globally, 10 billion tonnes of chitin have been biosynthesised and 1.5 million tonnes of chitins are commercially available.<sup>65</sup> Chitin is a linear polysaccharide first identified in 1884, made up of (2-amino-2-deoxy-D-glucose) D-glucosamine and N-acetyl-2-amino-2-deoxy-D-glucose (N-acetyl-D-glucosamine) units which are linked by 1–4- $\beta$ -glycosidic bonds and it is the only source of chitosan. Structurally, the N-acetyl-2-amino-2-deoxy-D-glucose monomer is largely found in chitin, whereas the concentration of 2-amino-2-deoxy-D-glucose is high in chitosan. Chitin/chitosan are semi-crystalline in nature due to the presence of inter- and intramolecular hydrogen bonding. Chitosan is generally obtained by the deacetylation of chitin.<sup>66</sup> In 1894, Hopper demonstrated deacetylated chitin using potassium hydroxide solution, later named chitosan.<sup>67</sup> Significantly, in acidic pH, protonated ammonium ( $pK_a$  ( $-NH_3^+$ ) = 6.3) disrupts the crystalline nature of chitosan, leading to the solubilization of the polymer in an aqueous medium. In fact, chitosan is the only cationic polymer available in nature and is the only commercially available water-soluble cationic polymer, which makes it an important candidate in designing various sustainable functional materials.<sup>68</sup> Chitosan containing hydroxyl groups and reactive amine functionality in its structure is extensively utilised to prepare high-performance functional materials in a desired physical form

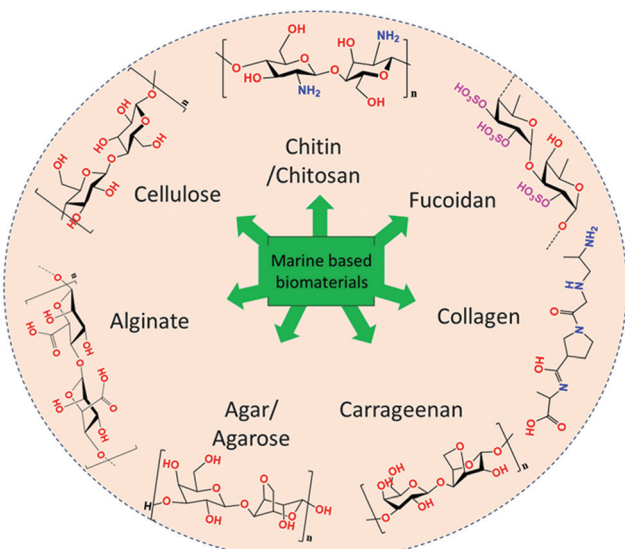


**Fig. 3** Various biomacromolecules derived from marine biomaterials and their chemical structures.

due to its water solubility. It readily interacts with charged organic and inorganic species through electrostatic interaction, coordination, metal-ligand interaction and through weak van der Waals forces or hydrogen bonding. Altogether chitosan can be considered an eco-friendly complexing agent because of its renewability, economic cost, nontoxicity, hydrophilicity and biodegradability.<sup>69</sup>

Further, its chemical properties, such as being a polyelectrolyte at acidic pH, high reactivity, coagulation, flocculation and biosorption properties, resulting from the presence of reactive hydroxyl and mostly amine groups in the macromolecular chains make it a most prominent candidate for water purification applications. In 1969, Muzzaiulli discovered that chitosan can collect natural heavy metal ions from seawater by a chelating effect.<sup>70</sup> In 1974, Friedman and group systematically explored the metal ion binding capacity of chitosan for the first time along with other biopolymers,<sup>71</sup> while the application of chitosan in wastewater treatment was demonstrated in 1976.<sup>69,72,73</sup> Since then extensive research has been carried out to develop efficient low-cost chitin/chitosan-based materials for water purification, especially as adsorbents for the separation of organic and inorganic contaminants (Fig. 5).

Over the past few decades, chitosan being a cationic biopolymer has received a great deal of attention for coagulation-flocculation processes due to its ability to form polyelectrolyte complexes in an aqueous medium.<sup>74,75</sup> Chitosan was successfully demonstrated for the flocculation of kaolin suspension,<sup>76</sup> algal cells,<sup>77,78</sup> river silt,<sup>79</sup> humic acid solution,<sup>80</sup> *Chlorella*,<sup>81</sup> tetracycline,<sup>82</sup> dyes,<sup>83</sup> pesticides,<sup>84</sup> heavy metal ions<sup>85</sup> etc. Various modified chitosans, such as chitosan glutamate, chitosan hydrochloride, and carboxymethyl chitosan, exhibited excellent contamination removal due to effective interaction with pollutants.<sup>80,86</sup> A study also demonstrated that a chitosan composite exhibited a higher percentage of removal compared to commercially applied flocculants, such as polyaluminum chloride and silicate for organic contaminants and solid suspended particles in water treatment.<sup>55</sup> Thus, chitosan has

been widely explored because the process is efficient even at low dosage, with a quicker depositing velocity, easier sludge treatment, and biodegradability and it exhibited high efficiency in coagulating and flocculation organic matter, inorganic ions and solid particles.<sup>87,88</sup> Interestingly, chitosan was also used for the flocculation of oil-water emulsion attributed to the hydrophilic nature of chitosan, which is explained in a later part of the review (section 3.3).

### 3.1 Decontamination of organic contaminated water

Over the past few decades, textile, pharmaceutical and many other industries have raised serious concerns as they have been releasing organic contaminants, such as dyes, pharmaceutical drugs, pesticides, surfactants etc., containing untreated wastewater into the environment, which has caused severe health issues to human beings, and terrestrial and aquatic living organisms.<sup>89,90</sup> Interestingly, chitosan-based beads,<sup>91</sup> thin films,<sup>92</sup> biocomposite membranes,<sup>93</sup> hydrogels and aerogels<sup>94</sup> were widely explored for the separation of such organic contaminants. The amine functionality in the chitosan intensely remains as an active site for the adsorption of organic moieties depending on the pH of the reaction medium.<sup>95</sup> Further, with an increase in the amine functionalities, diminishing the degree of acetylation enhances the adsorption of dye molecules. Thus, various modifications of chitosan were achieved by (i) crosslinking reactions with multi-functional moieties and (ii) grafting of highly functionalised monomers or polymers.<sup>96</sup> Both techniques yield chitosan derivatives with superior properties, such as improved surface functionality, enhancement of active sites, and also physical, chemical and thermal stability.<sup>97</sup> In the case of grafting, auxiliary chemicals are required to form a stable composite with chitosan, whereas crosslinking may lead to reduced functionalities. The functionalities of chitosan have been enhanced by grafting with various chemicals—such as poly(methyl methacrylate),<sup>98,99</sup> diethylene triamine,<sup>100</sup> polypropylene imine,<sup>101</sup> sulfonic acid,<sup>102</sup> and  $\beta$ -cyclodextrin,<sup>103,104</sup> and also with nanomaterials, such as graphene oxide (GO),<sup>105</sup> reduced graphene oxide (rGO),<sup>106,107</sup> and single-walled and multi-walled carbon nanotubes (SWCNT & MWCNT)<sup>108,109</sup>—further, establishing their application in water purification.

Over past decades, exfoliated graphene oxides have been extensively studied due to their excellent adsorption capacity attributed to huge polar moieties, such as epoxy, hydroxy, and carboxy groups and high surface area.<sup>110–112</sup> A group led by Prof. Saleh has established the use of GO for various applications, such as powerful adsorbents,<sup>113</sup> sensors,<sup>114</sup> photocatalysts,<sup>115</sup> and also as a filler in membranes<sup>116</sup> to treat the water obtained as a by-product of the petrochemical industry.<sup>117–119</sup> Thus, graphene oxide was widely utilised to prepare chitosan composites for water purification applications. By stacking into a continuous membrane, GO with a two-dimensional lamellar structure and single-atom thickness has shown advantages in water purification.<sup>120–122</sup> Chen *et al.* have prepared a GO-chitosan hydrogel through self-assembly of GO within a chitosan network. The hydrogel exhibited enhanced

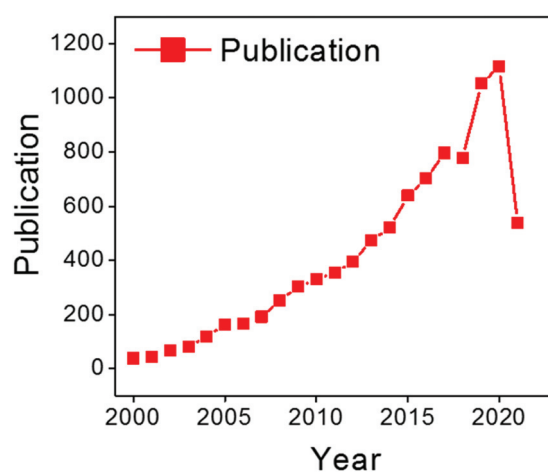


Fig. 5 Distribution of publications on chitosan for adsorption per year according to the Web of Science from 2000 to July 2021.

adsorption through a column filtration mode for a comparison of cationic and anionic dyes. It is also observed that the performance increases with an increase in GO content.<sup>123</sup> Later, Kamal *et al.* demonstrated tetraethyl orthosilicate crosslinked GO/chitosan film for Congo red dye separation with excellent adsorption capacity.<sup>124</sup> Interestingly, the GO/chitosan composite shows robust separation of organic dyes under ultra-sonication, which is advantageous in a real-time scenario.<sup>125</sup>

Recently, GO/chitosan aerogels with high mechanical strength were demonstrated for the separation of various organic contaminants.<sup>126,127</sup> On the other hand, the development of magnetic composites has attracted various research groups around the globe. It is suggested that a magnetic property can be enabled by incorporating magnetic composites like  $\text{Fe}_3\text{O}_4$  into the chitosan network. The chitosan forms stable composites with metal composites through metal-ligand interaction with the hydroxyl and amine groups. The magnetic composites can be prepared by both *in situ* and *ex situ* processes.<sup>107,128</sup> Efforts were made to enhance adsorption by grafting with cyclodextrin<sup>129</sup> and GO<sup>130</sup> along with magnetic composites. The hydrophobicity and surface functionality of cyclodextrin and GO enhance the adsorption capacity of chitosan. Advantageously, chitosan exhibits antibacterial activity by binding to the negatively charged bacterial cell wall, causing disruption of the cell. Thus, magnetic chitosan/GO composites demonstrated antibacterial activity against *Escherichia coli* from an aqueous medium.<sup>131</sup> Further, the antibacterial property was enhanced by introducing silver nanoparticles into the chitosan network through the photocatalytic reduction of silver nitrate, and the composite was used for adsorption of various dye molecules.<sup>132</sup> Recently, chitosan-based novel magnetic nano-adsorbents in the fluid state were prepared *via* a facile *in situ* co-precipitation method. The magnetic adsorbent exhibited robust separation and superior adsorption capacity of  $1724 \text{ mg g}^{-1}$  for Congo red dye and was easily recyclable with magnetic assistance.<sup>133</sup> Further, various chitosan-based hydrogels and aerogels were demonstrated for organic contaminant separation.<sup>134,135</sup> Among them, aerogels are promising candidates due to high active surface contact with the pollutants and easy implementation.

A polydopamine-modified chitosan-based aerogel was reported for the separation of organic dyes along with heavy metal ions.<sup>136</sup> The enhanced adsorption is attributed to the large number of amine and catechol groups on its molecule. Similarly, polydopamine-modified carboxymethyl cellulose-based aerogel was also evaluated for cationic and anionic dye separation.<sup>137</sup> Also, low-cost fly-ash and GO-immobilised chitosan aerogel were explored for reactive orange 16 dye, which exhibited moderate adsorption.<sup>138</sup> Fly-ash is a low-cost mineral residue obtained after burning charcoal in an electricity generating plant.<sup>139</sup> Chitosan was also used to exfoliate a phyllosilicate, and further crosslinked with rGO to form a porous hydrogel with remarkable mechanical strength without the aid of a crosslinker (Fig. 6).<sup>140</sup> Further the porous hydrogel was used for chromium separation. Recently, our group has reported iron and aluminium composite-functionalised adsorption-

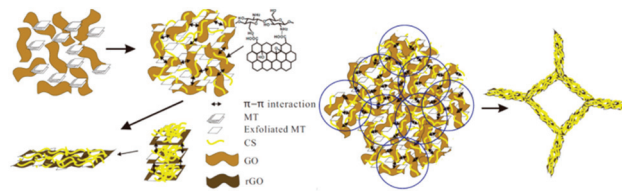


Fig. 6 Schematic representation of the fabrication of a composite hydrogel with a porous structure.<sup>140</sup>

based aerogel membranes for dye, pharmaceutical and pesticide separation.<sup>141</sup> These studies suggested that economical aerogels can be prepared by functionalising chitosan aerogel for the efficient decontamination of organic wastewater.

On the other hand, photodegradation and advanced oxidation processes (AOPs) are promising wastewater treatment technologies which are widely used around the world.<sup>142,143</sup> Various research groups have demonstrated chitosan-based catalysts for the degradation of organic pollutants *via* photodegradation<sup>144</sup> or AOPs.  $\text{TiO}_2$ ,<sup>145,146</sup>  $\text{Ag}$ <sup>147</sup> and  $\text{ZnO}$ <sup>148,149</sup> immobilised chitosan composites were widely used for photocatalysis.  $\text{TiO}_2$  is an n-type semiconductor initiating photocatalytic oxidation at a wavelength of 320 nm. Thus,  $\text{TiO}_2$ -impregnated chitosan composites were widely developed for the degradation of various organic contaminants. Zainal *et al.* cast a  $\text{TiO}_2$ -chitosan composite based thin film over a glass support and examined its photocatalytic activity.<sup>150</sup> The composite showed excellent removal of model organic contaminants *via* the combined effect of adsorption and photodegradation. Later,  $\text{TiO}_2$ -encapsulated chitosan beads and surface-imprinted beads were developed for a continuous photocatalytic mode of organic dye and pesticide degradation.<sup>146,151</sup> In general, emerging contaminants such as pharmaceutical drugs are difficult separate through adsorption or membrane filtration, so degradation is the most suitable technique for such contaminants.<sup>151,152</sup> Apparently, the surface-decorated composite shows robustness due to the greater exposure of active sites. However, there is a high chance of the leaching of nanocomposite deposited over the surface during the impregnation treatment, which harms the recyclability and also induces additional pollution into the system. Recently, catalysts for AOPs were also developed, such as a Fenton catalyst,<sup>153</sup> cobalt oxide,<sup>154</sup>  $\text{ZnS}$ <sup>155</sup> and ferrocene<sup>156</sup> functionalised chitosan materials. However, they are still limited to lab-scale demonstrations due to the requirement of a high loading of active catalyst and the consumption of a large amount of peroxide and persulfate chemicals.

Membrane technology is widely used for wastewater treatment, drinking water treatment and desalination due to its low production cost, operational simplicity and ease of scaling up.<sup>157</sup> However, conventional membranes are mostly derived from petroleum-derived polymers or synthetic polymers which exhibit threats to the environment after disposal. Moreover, conventional membranes suffer from biofouling and low permeability.<sup>158</sup> Chitosan has gained increasing interest as a

membrane material due to its hydrophilicity, ease of modification, biocompatibility, and remarkable affinity to organic molecules and inorganic metals. Over the past two decades various chitosan-based crosslinked and composite membranes have been widely developed for wastewater treatment.<sup>93</sup> Evidently, functionalisation or modification of chitosan polymer significantly enhance the performance; thus, various crosslinking agents, such as organic molecules,<sup>159–162</sup> metal salts<sup>163–165</sup> and inorganic acids,<sup>166</sup> have been demonstrated. The crosslinking causes shrinkage of the polymer, which leads to a reduced porous structure helping in the high removal of pollutants; however, it also reduces the flux rate. On the other hand, composite membranes can be produced by blending with synthetic polymers,<sup>167</sup> biopolymers, metal composites, carbonaceous materials<sup>168</sup> etc. The blending of two oppositely charged polymers leads to polyelectrolyte complexes. Since chitosan is the only cationic polymer, it has been widely used to prepare biocompatible polyelectrolyte complexes with alginate, carboxylate cellulose, poly(acrylic acid) (PAA) and other anionic polymers. The blending leads to highly selective water permeability with enhanced mechanical and thermal stability. To enhance the hydrophilicity of the membrane, chitosan was blended with poly(vinyl alcohol) (PVA), alginate, poly(ethylene glycol) etc. Whereas a hydrophobic membrane was obtained by blending with polysulfone, polyacrylonitrile, polyvinylidene-fluoride etc. Thus, according to the nature of the pollutant, monomers or polymers were selected for desired molecular separation.

Recently, there has been a growing interest in developing thin film composite (TFC) membranes due to their advantages, such as anti-fouling property and enhanced recyclability. TFC membranes consist of an active thin layer formed by interfacial polymerisation which determines the performance of a membrane and a macro-porous support which gives it mechanical strength.<sup>93,169,170</sup> Commercially, a polyamide membrane is a widely used TFC membrane due to its remarkable mechanical strength, but it suffers from low flux and biofouling, which led to efforts to replace the polyamide layer, with limited success.<sup>171,172</sup> Recently our group has successfully demonstrated silver crosslinked chitosan as an active layer over a polysulfone membrane (Fig. 7). The chitosan-based membrane not only exhibits anti-fouling propensity, it also showed a superior pure water flux of  $100 \text{ L m}^{-2} \text{ h}^{-1}$  (LMH).<sup>174</sup> The membrane exhibited >98% rejection for dyes and tannery wastewater with a flux rate of up to 30 LMH. Further, the flux and rejection of the membrane were enhanced by immobilising a spiral-like carbonaceous material in the active chitosan layer.<sup>173</sup> Interestingly, the multifunctional helical structured carbon acts as a crosslinker, a hydrophilic membrane filler which led to the superior membrane performance. Thus, a chitosan-based membrane could be a potential membrane for an effective pre-treatment of various industrial organic wastewaters.

### 3.2 Decontamination of inorganic contaminated water

Heavy metal ions are very toxic/hazardous and should be eliminated from wastewater and drinking water. Heavy metals are

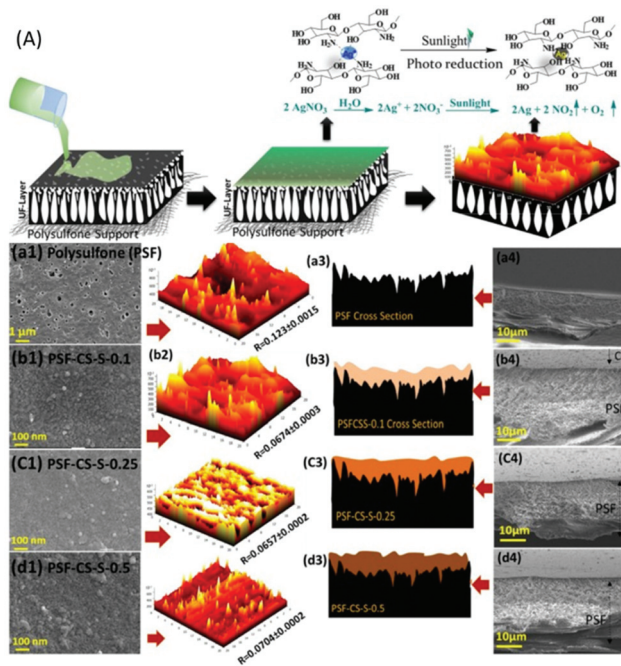


Fig. 7 (A) Schematic representation of the fabrication of a chitosan-based thin film membrane over a polysulfone support. (a–d) SEM, AFM analysis, schematic representation and cross-section of the membrane showing the surface topology and the roughness of the membrane with varying concentrations of chitosan.<sup>174</sup>

generally the group of metals/metalloids with an atomic density of more than  $4000 \text{ kg m}^{-3}$ .<sup>175</sup> Many processes are conventionally used for the removal of heavy metals from water and wastewater; however, trace concentrations of heavy metals in effluents remain a great concern where restrictive standards should be passed before discharge. Various operations, including ion exchange, flotation, electro-coagulation, solvent extraction, membrane filtration, and adsorption have been used for the elimination of metals from aqueous environments.<sup>176</sup> Among them, the adsorption technique is the most widely studied phenomenon due to the ability of chitosan to form coordinate or metal-ligand interactions with the heavy metal ions and inorganic anions attributed to its enormous amine and hydroxyl functionality, which also helps in the recovery of heavy metal ions.<sup>91,177</sup> Chitosan and its derivatives are the most promising adsorbents for the separation of heavy metal ions, such as As(III/V), Fe(II/III), Pb(II), Cr(VI), Cu(II), Ni(II), Hg(II), Ag(I) etc., and inorganic nutrients, such as nitrate, sulfate, fluoride, chloride etc. Further, they have been extensively reviewed for their separation efficiency.<sup>29,90,178–181</sup> Thus, the present section provides a brief explanation of the various strategies for preparing high-performance adsorbents for metal ions and inorganic nutrients.

For various chitosan-based crosslinked materials, such as beads, hydrogels, aerogels, polymeric composites, grafting a functional group onto them was widely demonstrated to synthesise an efficient adsorbent for the adsorption of inorganic contaminants.<sup>182–184</sup> Glutaraldehyde, epichlorohydrin and

ethylene glycol diglycidyl ether are the most commonly used crosslinkers for chitosan. However, crosslinking of chitosan generally leads to a non-porous macrostructure and diminished functionalities which limits their adsorption capacity.<sup>90,185</sup> This is because the hydroxyl groups and amine functional groups react with the crosslinker, leading to a decrease in active adsorption sites. Further, researchers have developed a low-cost grafting method for the preparation of high-performance hybrid materials. The modification of chitosan led to an increase in surface functionality, which is crucial for the adsorption technique. Monomers like succinic acid, acrylic acid and itaconic acid were used to graft carboxyl groups onto the chitosan.<sup>186</sup> Ethylene diamine tetra acetate, thiourea and cyclodextrin are the other popular grafting agents for chitosan.<sup>96,187</sup> By tuning the pH with respect to the  $pK_a$  value of a composite, cationic and anionic pollutants can be selectively adsorbed over the composites. Chitosan-based hybrids were also prepared with biomaterials such as nano-clays, silica, cellulose, agarose, alginate, polyvinyl alcohol, and nanofibrils.<sup>96,188,189</sup> These composites enhance the functionalities, and induce mechanical strength and also chemical stability. Due to the high functionality, heavy metal ions were successfully separated from an aqueous medium through electrostatic interaction. Another important strategy is to introduce carbonaceous materials, such as GO, rGO, CNT, hydrothermal and activated carbons.<sup>190–192</sup> Due to a synergistic combination of the high surface area of carbonaceous materials and the high functionality of chitosan or chitosan derivatives, they provide superior adsorption of inorganic contaminants.<sup>193</sup>

On the other hand, extensive efforts have been made to immobilise active metal composites, such as iron, aluminium, zirconium, silver, or molybdenum, into the chitosan network. Interestingly, chitosan has the ability to bind colloidal nanoparticles in the ratio 500 wt%/wt% attributed to its enriched multifunctionality.<sup>194</sup> The synergistic combination of active metal composites and chitosan has shown superior adsorption capacity for various contaminants. Significantly, metal/chitosan composites were commercialised thanks to their low cost, biodegradability and excellent recyclability. For example, Pradeep and group demonstrated an antimicrobial composite made by immobilizing silver nanoparticles and ALOOH into the chitosan network.<sup>194</sup> Interestingly, the polymeric network was developed for the controlled release of silver nanoparticles, which helps in the decontamination of pathogens; further, ALOOH successfully scavenged arsenic, lead and iron ions. They also developed and commercialised an FeOOH-chitosan composite for real groundwater contaminated by arsenate and ferric ions and demonstrated it as a point-of-use filter for drinking water in various parts of India.<sup>195</sup> The chitosan not only effectively immobilised the metal nanocomposites, it further exhibited the controlled release of silver nanoparticles for antibacterial activity. Interestingly, these composites also exhibited a remarkable adsorption capacity for fluoride; however their performance was hindered by the presence of co-anions such as phosphate, nitrate and chloride.<sup>196</sup> Inspired by this, we have designed and developed an  $\alpha$ -FeOOH and

$\gamma$ -ALOOH functionalised chitosan-based ultrafast permeable, hydrophilic aerogel for scavenging fluoride from contaminated groundwater (Fig. 8A).<sup>141</sup> The aerogel successfully purified 4734 L of fluoride-contaminated groundwater (Fig. 8B), and further exhibited a maximum adsorption capacity of 102 mg g<sup>-1</sup> for arsenic and 81.5 mg g<sup>-1</sup> for fluoride. Researchers have also developed magnetic composites because of their many advantages like easy collection of adsorbents from an aqueous medium and enhanced adsorption of metal ions due to the magnetic property.<sup>197–200</sup> Further, the selective separation of metals of inorganic contaminants can be achieved by ion-imprinting technology. The process involves adding a target template ion into the chitosan solution prior to crosslinking followed by removal of the template ion.<sup>201–203</sup> The created void will selectively adsorb the targeted ions.

### 3.3 Oil-water separation

The escalating discharge of industrial oily-wastewater and frequent worldwide occurrence of oil-spillage accidents demand highly efficient materials for oil-water purification. Over the past few decades, various physical and chemical treatments have been established to separate oil from water.<sup>204,205</sup> Flocculation is one such type of chemical treatment, where chemical agents separate the oil-water mixture by destabilization of the oil-water emulsion *via* neutralising the surface charges of the emulsion droplets. However, the process requires a huge amount of chemicals, and thus requires low-cost, biodegradable and nontoxic demulsifiers and flocculants.<sup>206</sup> The polyelectric nature and higher charge density of

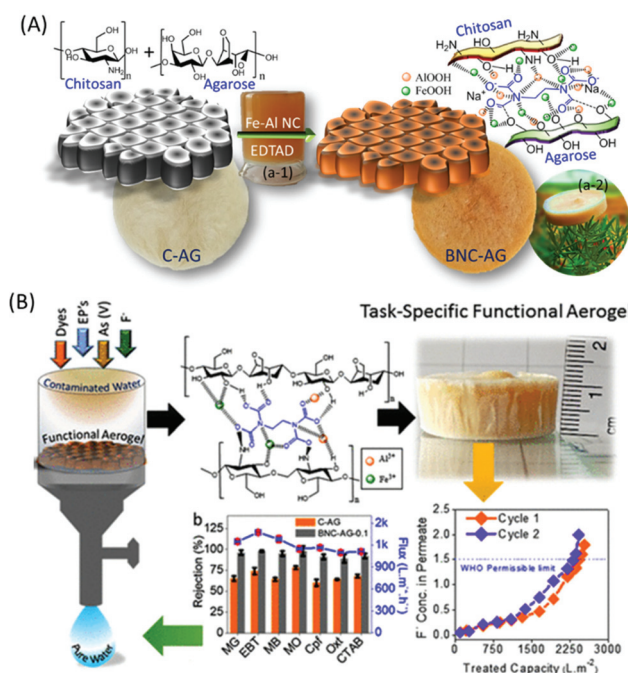


Fig. 8 (A) Fabrication of iron and aluminium based composite functionalised aerogel and (B) performance of the aerogel membrane for the separation of dyes, pharmaceutical drugs, surfactants and fluoride ions from an aqueous medium.<sup>141</sup>

chitosan in an acidic medium assist the efficient flocculation of oil from an oil–water emulsion.<sup>206</sup> The flocculation is dominant due to charge neutralization instead of bridging. Thus low-cost chitosan-based flocculant exhibited greater efficacy than traditional coagulants, such as alum or polyaluminum chloride.<sup>206</sup>

Chitosan exhibits up to 99% separation of oil from palm oil mill effluent due to the synergistic combination of adsorption, effective agglomeration and coagulation. Further, hydrophobically modified chitosan enhances the separation of oil from sodium dodecyl sulfate stabilised oil–water emulsion attributed to its hydrophobicity and surface functionalities.<sup>207</sup> However, the cost of chitosan is high compared with most inorganic flocculants, which restricts its commercialisation.<sup>208</sup> Zhang *et al.* prepared a hydrophilic, underwater superoleophobic, anti-oil-fouling chitosan/PVA based mesh inspired by shrimp shells.<sup>222</sup> More than 99% separation was achieved through a gravity-driven filtration system with or without hyper-salinity. Interestingly, enhanced performance was observed with a silica-impregnated chitosan mesh attributed to the high surface area of the silica composite. Later, a bio-polymer aerogel system has emerged as a prominent functional material for the separation of an oil–water emulsion. Meena and co-workers have demonstrated a highly crosslinked chitosan/agarose-based biohybrid aerogel membrane for the efficient separation (>99%) of water from real oil-spill wastewater collected from a shipbreaking yard (Fig. 9a–c); further preparation and application of the biobased aerogel process were patented.<sup>210,211</sup> The chitosan acts as a support network and provides hydrophilic channels for water to pass through it (Fig. 9d–f). Thus, a flux rate of up to 600 LMH with >99% rejection was obtained in a crossflow membrane filtration mode. Similarly, various attempts were made to prepare an aerogel using superhydrophilic<sup>209</sup> and superhydrophobic<sup>212</sup> modified chitosan. Also, hybrid aerogels were prepared using alginate,<sup>213</sup> cellulose,<sup>214</sup> polydopamine<sup>212</sup> etc. to enhance the mechanical strength, chemical stability and permeability of the aerogel membrane. Interestingly, nanocomposites such as GO and TiO<sub>2</sub>-impregnated aerogel membranes, enhance oil-absorption,<sup>215</sup> and induce a self-cleaning property in the aerogel membranes.<sup>215</sup> Recently, we have demonstrated an Fe-Al composite functionalised chitosan aerogel exhibiting >99% separation of an oil–water emulsion with ultrahigh permeation attributed to the superhydrophilic nature of chitosan.<sup>141</sup> Herein, the metal composites not only enhance the hydrophilicity of the membrane but also enable multifunctional properties. Interestingly, one can tune the path structure for liquid transport through unidirectional freeze drying.<sup>216,217</sup> In sum, low-cost, biodegradable chitosan-based membrane are promising candidates for practical oil–water separation applications.

### 3.4 Solar-assisted water evaporation

Solar-assisted water distillation is a promising facile technique to produce fresh water. Recently, there has been an increase in attention paid to developing highly efficient solar-thermal

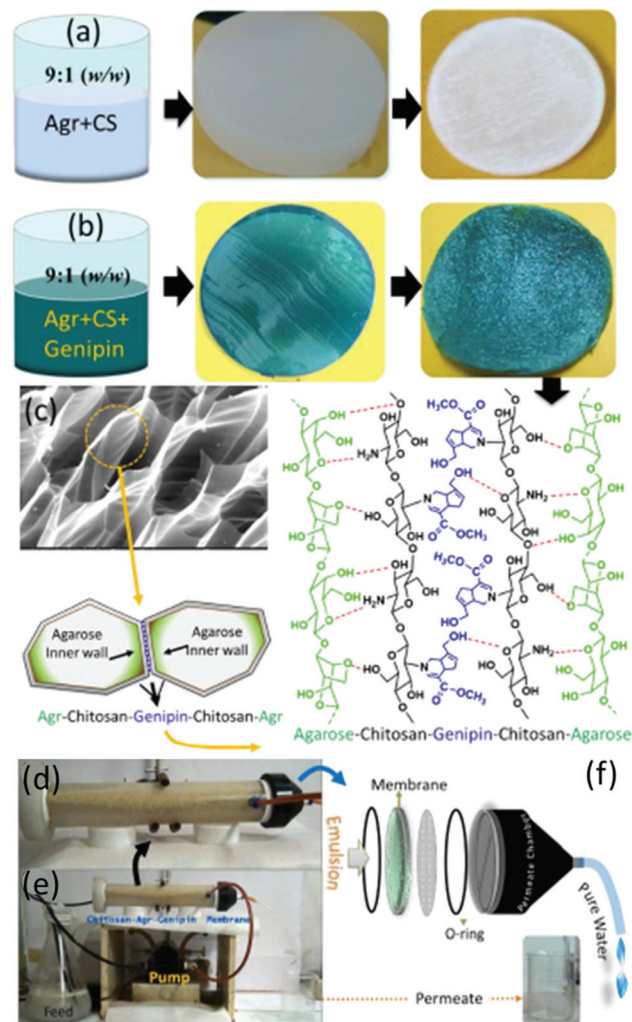


Fig. 9 (a–c) Schematic and digital images of highly crosslinked, superhydrophilic agarose/chitosan aerogel. (d–f) Cross-flow membrane filtration of crude oil based emulsion separation.<sup>210</sup>

conversion materials for water evaporation. In a general strategy, researchers have immobilized a highly efficient solar-thermal converter catalyst in a high surface area matrix. In this regard, chitosan is a perfect candidate since the high surface functional groups can efficiently accommodate nanocatalysts and its natural hydrophilic nature will enhance the water permeability throughout the system. Zhou *et al.* designed highly hydratable polymeric hybrid hydrogels using PVA and chitosan.<sup>218</sup> Conductive polypyrrole was infused as a light-absorbing catalyst. The hydrogel exhibits a superior water evaporation rate of  $3.6 \text{ kg m}^{-2} \text{ h}^{-1}$  under 1-sun illumination. Likewise, Wang *et al.* substituted PVA with polyacrylamide and obtained a similar conversion efficiency; however, it showed long-term stability against salt and bacterial accumulation.<sup>219</sup> Further, an rG-induced chitosan hydrogel was reported as a salt-resistant solar-thermal converter with an efficiency of 86% for water evaporation.<sup>220</sup> The induced rGO acts as a spacer and enhances the transport of water within the hydrogel system.

and also the compression strength. Wang *et al.* fabricated a double-layered GO-chitosan/ZnO scaffold for solar steam generation by keeping a GO layer on the top.<sup>221</sup> The hybrid aerogel exhibits a steam generation rate of  $13.5 \text{ kg m}^{-2} \text{ h}^{-1}$  under 10-sun illumination. Similarly, silver nanoparticles,<sup>222,223</sup> molybdenum carbide,<sup>224</sup> melanin-coated titania hollow nanospheres<sup>225</sup> and  $\text{MnO}_2$  nanowires<sup>226</sup> immobilised chitosan-based materials were examined for solar steam generation. In sum, these low-cost, highly efficient advanced materials show potential applications in practical solar-driven wastewater treatment.

## 4. Alginate

Alginate is an anionic polysaccharide extracted from the component of the cell walls of brown algae and an exopolysaccharide of some bacteria such as *Pseudomonas* and *Azotobacter*. To be more specific, it is a copolymer of  $\alpha$ -L-guluronic acid and  $\beta$ -D-mannuronic acid linked together by  $\beta$ -1,4-glycosidic bonds.<sup>227</sup> Commercially, alginate is produced using *Laminaria hyperborea*, *Laminaria digitata*, *Laminaria japonica*, *Ectonia maxima*, *Macrocystis pyrifera*, *Durvillea Antarctica*, *Lessonia nigrescens*, and *Sargassum* spp.<sup>228</sup> Alginate salts are generally water soluble, possess an excellent gelling property and are hydrophilic in nature due to extensive hydroxyl and carboxylic functionalities. Thus, they are extensively utilized in wastewater remediation, which is further attributed to their structural stability, high water permeability, biodegradability, and nontoxic nature.<sup>229</sup> Interestingly, numerous studies have indicated that the efficiency of alginates can be improved by developing hybrids with suitable materials. Over the past decade, alginate-based hybrid materials have been developed using synthetic polymers, biopolymers and inorganic metal salts or composites which yielded multi-functional beads, hydrogels, aerogels and membranes for efficient water purification.<sup>230</sup> Such various strategies used to develop high-performance materials are discussed here.

### 4.1 Decontamination of organic contaminated water

It was observed that alginate plays a critical role in the biosorption efficiency or ion-exchange capacity exhibited by brown seaweeds.<sup>38</sup> This suggested that alginate would be an excellent candidate for sorption application. In the late 20<sup>th</sup> century, researchers studied the biosorption and adsorption efficiency of alginate and its hybrids mainly for heavy metal ions<sup>231–233</sup> and for some organic contaminants.<sup>234,235</sup> Later, over the past two decades, alginate-based materials have attracted immense research interest due to their chemical stability and biocompatibility. Calcium alginates are the most studied materials for adsorption; however, generally they are non-porous and exhibit a limited surface area.<sup>236</sup> Thus, many strategies—such as gelation with boehmite,<sup>237</sup> incorporation of surfactants and porogens such as  $\text{NaCl}$ ,  $\text{CaCO}_3$ ,<sup>238</sup> and preparing composites with various biomaterials such as nanoclays<sup>239</sup>—were demonstrated to prepare porous alginate materials. Surfactants such as

sodium dodecyl sulfate<sup>240</sup> or cetyltrimethylammonium bromide<sup>241</sup> create a porous structure through non-spherical simultaneous micelles which act as a pore-forming template in alginate hydrogels. Further, grafting of alginate composites is another important technique to obtain high-performance materials. Various monomers and polymers were used, such as acryl amide,<sup>242</sup> tannic acid,<sup>243</sup> cyclodextrin, polyacrylamide,<sup>244</sup> PVA,<sup>245</sup> itaconic acid *etc.* to enhance the efficiency of alginate-based materials.

Shao *et al.* have demonstrated 2-acrylamido-2-methylpropano-1-propanesulfonic acid grafted over sodium alginate through hydrogen bonding for the ultrahigh adsorption of methylene blue, which showed a maximum adsorption capacity of  $2977 \text{ mg g}^{-1}$ .<sup>246</sup> Whereas, a polyethyleneimine-grafted MXene incorporated double-network structured alginate aerogel exhibited an ultrahigh adsorption of  $3568 \text{ mg g}^{-1}$  for Congo red dye.<sup>247</sup> Similarly,  $\text{ZnO}$ -impregnated PAA-grafted alginate hydrogel and  $\text{TiO}_2$ -impregnated acrylic-acid-grafted alginate hydrogels<sup>248</sup> have shown superior adsorption capacities of  $1539 \text{ mg g}^{-1}$  and  $2257 \text{ mg g}^{-1}$  for cationic methylene blue dye, respectively, attributed to electrostatic interaction between the carboxyl groups of grafted alginate and the high surface area of  $\text{ZnO}$ .<sup>249</sup> Furthermore, various hybrid composites have been prepared by incorporating GO, rGO, CNT,<sup>250</sup> or activated carbon<sup>251</sup> into the polymeric network to enhance the sorption capacity. A high specific surface area, surface functionality and mechanical stability enhance the performance of alginate-based materials for the separation of dyes, pharmaceutical drugs and pesticides.

GO-functionalised alginate beads showed a maximum adsorption capacity of up to  $342.6 \text{ mg g}^{-1}$  for bisphenol A, which is several times higher than conventional adsorbents.<sup>252</sup> Recently, calcium-alginate-based membranes have shown a superior adsorption capacity of  $3506 \text{ mg g}^{-1}$  for methylene blue dye.<sup>253</sup> Significantly, silver-nanoparticle-incorporated alginate-based adsorbents were explored as a point-of-use microorganism disinfectant during the purification of drinking water.<sup>254</sup> Similar efforts were made to prepare metal composites<sup>255</sup> immobilized alginate composites, such as zeolite,<sup>256</sup> boehmite, goethite,<sup>256</sup> molecular organic frameworks,<sup>257</sup> and magnetic composites. Further, alginate-based catalysts for photocatalytic degradation and AOPs were also demonstrated. In 2000, iron-encapsulated alginate gel beads were demonstrated for the Fenton degradation of orange II dye. Later, in 2005, a chitosan-alginate-based polyelectrolyte microshell constructed *via* a layer-by-layer self-assembly technique was demonstrated for the photo-assisted Fenton degradation of dye molecules. Over the past decade a renewed interest was observed for the utilisation of alginate for photocatalysis. Efforts were made to immobilise  $\text{TiO}_2$ ,<sup>258,259</sup>  $\text{ZnO}$ ,<sup>260</sup>  $\text{g-C}_3\text{N}_4$ ,<sup>261</sup>  $\text{La}(\text{OH})_3$ ,<sup>262</sup>  $\text{Ag}_3\text{PO}_4$ ,<sup>263</sup> and  $\text{CuO}$ <sup>264</sup> into an alginate matrix and their photocatalytic activity was successfully demonstrated. Alginate acts as an efficient dispersive medium and controls the agglomeration of nanocomposite during self-assembly, thus facilitating an excellent degradation reaction. Hence, alginate could be a potential candidate for photodegradation and AOPs reactions.

#### 4.2 Decontamination of inorganic contaminated water

In general, sodium alginate can form an “egg-box structure” by interacting with multivalent metal ions through a sol-gel precipitation which yields polymer beads.<sup>265</sup> Specifically, multivalent metals like Ca(II) have the ability to form guluronate structures like eggs in an egg box, and the alginate chains bind them together with junction zones.<sup>266</sup> Over past decades, immense research has been conducted to develop highly functionalised, porous alginate-based materials for the robust separation of inorganic contaminants through adsorption<sup>267</sup> and membrane filtration.<sup>268</sup> Interestingly, reports have suggested that alginate shows higher adsorption of heavy metal ions than chitosan due to the large number of active adsorption sites.<sup>269,270</sup> Various factors affect the binding capacity and affinity of alginate towards heavy metal ions, such as the nature of the pollutants, their net charge, the morphology of the materials, pH, temperature and existing ions in the aqueous medium, and also the functionality and surface area of the materials. Calcium and iron crosslinked alginate-based materials showed a low adsorption capacity for heavy metal ions due to their non-porous surface and low specific surface area.<sup>271</sup> Thus, the majority of the work has focused on the modification of alginate by grafting, hybridising with organic or inorganic composites and blending with synthetic or biopolymers. Polyethylenimine-grafted alginate aerogels have exhibited an ultrahigh adsorption capacity for Cr(VI) of 431 mg g<sup>-1</sup>, whereas the addition of Mxene has enhanced it up to 539 mg g<sup>-1</sup>.<sup>247,272</sup> In another study, 2-acrylamido-2-methylpropa-1-propanesulfonic acid grafted sodium alginate showed a superior adsorption capacity of 2042 mg g<sup>-1</sup> for Pb(II) ions.<sup>246</sup> Acrylic acid or PAA grafting is the most successful modification strategy to enhance the adsorption capacity of alginate-based materials. PAA-sodium alginate nanofibrous hydrogels have exhibited an excellent adsorption capacity of 591.7 mg g<sup>-1</sup> for Cu(II) ions.<sup>273</sup> Significantly, a nanofibril-based membrane showed up to 99% separation efficiency with a flux rate of 868 LMH even in a more concentrated solution. It is observed that

the thickness of the membrane directly influences the separation efficiency, and excellent rejection was obtained for a membrane with a thickness of 200  $\mu\text{m}$ . Significantly, a 3D macroporous alginate/akaganeite composite aerogel was established as a point-of-use filter for arsenic separation from drinking water with a flux rate of 20–25 mL min<sup>-1</sup> under gravity.<sup>274</sup> The robust separation from the scaffold is attributed to the efficient adsorption capacity of akaganeite. Further, an GO/alginate-based yttrium-impregnated hydrogel has shown an excellent adsorption capacity of 288.9 mg g<sup>-1</sup> for fluoride.<sup>275</sup> Also, the hydrogel-based filter has shown excellent separation of fluoride in continuous filtration mode, attributed to a robust ion-exchange reaction between hydroxide groups and fluoride anions, which promises its application to treat fluoride-contaminated water. Yttrium-immobilized GO alginate hydrogels have also shown a maximum adsorption capacity of 273 mg g<sup>-1</sup> for As(V), ascribed to H-bonds, electrostatic interaction and  $\pi$ - $\pi$  interaction.<sup>276</sup> Recently, our group demonstrated an aluminium-composite-impregnated chitosan-alginate-based biomaterial scaffold with silver nanoparticles for drinking water and industrial wastewater purification (Fig. 10).<sup>277</sup> The aluminium composite provides active adsorption sites, whereas the silver nanoparticles afford an antibacterial property. Notably, the performance of the material was examined through commercializable models, such as teabag-like pouches and a column filter for the separation of fluoride and chromate ions.

#### 4.3 Oil–water separation

A superhydrophilic alginic-based polymer is a promising candidate for oil–water separation due to its affinity towards water and high absorption capacity. Moreover, alginate gels can be easily converted into porous aerogels by simple supercritical drying or freeze drying. Since alginate exhibits a salt-tolerant property in a marine environment, a group of researchers demonstrated a superoleophobic sodium alginate based aerogel for oil–seawater separation. However, they used cell-



Fig. 10 (a) Schematic representation of the preparation of an aluminium-composite-impregnated sodium alginate and chitosan-based biomaterial scaffold. (b) Shows the application of the bio-composite for the separation of dyes, Cr(VI) and fluoride through a teabag model and a continuous flow method.<sup>277</sup>

ulose nanocrystals as a filler in order to enhance the mechanical stability of the alginate aerogel. The hybrid aerogel successfully separated oil from an oil–seawater mixture with >99% efficiency along with remarkable recyclability.<sup>278</sup> Further, an alginate-based self-cleaning aerogel was reported by immobilising multifunctional  $\text{TiO}_2$ , which exhibited underwater oleophobicity and subsequently up to 99% oil–water separation efficiency.<sup>279</sup> Thus, the report successfully addressed the fouling issue by enabling the self-cleaning property. The adsorbed oil molecules can be photocatalytically biodegradable under sunlight, which leads to regeneration of the aerogel surface. Further, a chitosan/alginate hybrid hydrogel and an amphotolytic membrane were also demonstrated for oil–water separation.<sup>213,280</sup> The hydrogel was prepared by coating chitosan/alginate over a copper mesh and the membrane was obtained by subsequent freeze drying. Significantly, the membrane exhibited >99% oil–water separation efficiency with a flux rate of 680 LMH. Furthermore, efforts were made to produce a highly efficient, durable and renewable aerogel by the incorporation GO into the alginate network.<sup>281</sup> The aerogel exhibited underwater super oleophobicity with an oil–water separation efficiency of >99% with a superior flux rate of  $3.5 \times 10^3$  LMH. Thus, the results suggest that alginate-based aerogels could be a potential solution to cleaning up oil spillages in seawater.

## 5. Agar/agarose

Agar is the oldest employed phycocolloid which is soluble in boiling water and is mainly used in the synthesis of solid microbiological culture media. It is a hydrophilic polysaccharide extracted from certain red algae and is mainly composed of neutrally charged agarose and charged fraction agarpectin, a composition similar to starch. Commercially, agarose is produced using *Gelidium* sp. and *Gracilaria* sp. which exist as a supporting structure in the cellular walls of the seaweeds.<sup>282</sup> Among agarose and agarpectin, agarose is a gelling fraction and becomes soluble in near boiling water. Upon cooling, the polymeric chains self-assemble into helical fibers that ultimately aggregate to form a hydrogel.<sup>283</sup> Structurally, agarose is a linear polysaccharide with repetitive units of D-galactose and 3,6-anhydro-L-galactose, linked by alternating  $\alpha$ -(1,3) and  $\beta$ -(1,4) glycosidic bonds. The presence of active C-2 and C-4 hydroxyl groups makes it an excellent candidate for water purification.<sup>284</sup> Areco *et al.* immobilised *Ulva lactuca*, in an agar matrix for the biosorption of bivalent heavy metal ions such as copper, zinc, cadmium and lead.<sup>285</sup> The dead biomass was dispersed in an aqueous agar medium to prepare an alga/agar composite. However, suspended alga showed better separation efficiency in a fixed-bed assisted continuous flow medium compares to an alga/agar composite. This can be attributed to readily available, freely distributed functionalities of alga in suspended medium enabling superior biosorption. Efforts were made to prepare various organic and inorganic composites of carbon dots,<sup>286</sup> Fe,  $\text{Fe}_2\text{O}_3$ ,<sup>287</sup> hydroxyapatite<sup>288</sup>

and organic polymers with agar for the adsorption of pollutants. Li and his group have prepared magnetic agarose microspheres for the separation of radionuclides.<sup>287</sup> A stable  $\text{Fe}_2\text{O}_3$ /agarose composite was formed by chelation with metal ions and it exhibited maximum adsorption capacities of 1.15 mmol g<sup>-1</sup> and 1.27 mmol g<sup>-1</sup> for U(vi) and Eu(III) radionuclides. Chen *et al.* synthesised an Fe-agarose nanocomposite and demonstrated its application in the separation of trichloroethylene and Cr(vi).<sup>289</sup> The Fe NPs were uniformly distributed inside the agarose hydrogels and reduced Cr(vi) to Cr(III).

Various strategies were developed to prepare excellent agar/agarose-based hydrogels and aerogels for water purification applications. Rani *et al.* investigated the biosorption capability of agar-based hydrogel.<sup>290</sup> The hydrogel was prepared by free radical copolymerization of acrylamide and *N,N'*-methylene bis-acrylamide which exhibited a remarkable swelling behaviour of up to 550% and superhydrophilicity attributed to the hydrophilic nature of agar molecules. These two properties are the key factors for the biosorption of heavy metal ions. The hydrogel exhibited affinity in the order  $\text{Fe}^{3+} > \text{Mn}^{2+} > \text{Ni}^{2+} > \text{Cr}^{3+}$  depending on the atomic radius of the heavy metal ions. Further, the hydrogel also exhibits notable adsorption of methylene blue dye. Interestingly, enhanced dye adsorption was observed from GO-immobilised agar hydrogel.<sup>291</sup> This is due to the enriched active sites and high surface area of the GOs. Seow *et al.* prepared an agarose-based superhydrophilic aerogel by simple freeze drying. The aerogel exhibited considerable adsorption capacity; however, its mechanical strength is unclear.<sup>283</sup> In 2014, our group demonstrated a highly crosslinked, novel superhydrophilic agarose/gelatine (9 : 1) based aerogel for sustainable oil–water emulsion separation.<sup>210</sup> The genipin crosslinks the cylindrical agarose chain, and phases were separated by non-crosslinked gelatine co-gel. Subsequently, gelatine forms a hydrogen bond with the agarose, which is confirmed by colour changes in the hydrogel. Upon freeze drying, the readily formed ice crystals in the agarose walls sublimated to form hydrophilic channels (Fig. 11).<sup>211</sup> As a result, the aerogel membrane exhibited a remarkable rejection of >99% with a flux rate up to 500 LMH

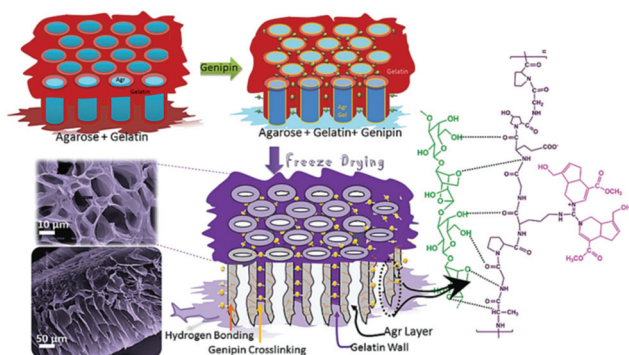


Fig. 11 Schematic representation of genipin crosslinked agarose–gelatine hydrogel formation and superhydrophilic, porous biobased aerogel membrane formation.<sup>211</sup>

for the cross-flow mode oil–water emulsion separation and aqueous–organic solvent mixture.

Recently, Wang *et al.* fabricated a fluorinated, superoleophilic agarose/GO hybrid aerogel with microchannels for the selective absorption of oil. Superhydrophobicity induced by fluorine functionalization enhances the organic solvent absorption up to  $187 \text{ g g}^{-1}$ . Interestingly, rGO-impregnated agarose hydrogel beads also exhibit superior adsorption of water-soluble organic moieties, including pharmaceutical drugs attributed to  $\pi$ – $\pi$  interaction with rGO.<sup>292</sup> The GO interaction with the carboxyl group of the agarose enabled better dispersion of hydrophobic GO by avoiding aggregation; on other hand, GO acts as a crosslinker to form water-stable agarose beads. The rGO/agarose composite beads exhibit a maximum adsorption capacity of  $321.7 \text{ mg g}^{-1}$  for Rhodamine B and  $196.4 \text{ mg g}^{-1}$  for aspirin. Whereas the GO/agar-based aerogel with GO content up to 80% exhibits a maximum adsorption capacity of  $578 \text{ mg g}^{-1}$  for methylene blue dye with excellent recyclability.<sup>293</sup> Agarose aerogel were also used in membrane distillation application. Aerogel will assist in reducing surfactant wetting by avoiding contact of the active membrane with the highly concentrated surfactants.<sup>294</sup>

Recently, a functional double-layer silver-poly(sodium-*p*-styrenesulfonate)-agarose gel/agarose gel was demonstrated for solar-assisted water evaporation (Fig. 12).<sup>295</sup> The silver-functionalised active agarose top layer induces a solar light-thermal transformation whereas the bottom hydrophilic agarose gel acts as an efficient water-transport medium, leading to excellent water vaporisation of up to  $2.1 \text{ kg m}^{-2} \text{ h}^{-1}$  under 1-sun illumination. Further, agarose-based hybrid materials were developed with carrageenan,<sup>296</sup> polyurethane,<sup>297</sup> polyvinyl alcohol,<sup>298</sup> and maltodextrin<sup>299</sup> for the separation of organic contaminants and also for catalytic reduction. Agar/agarose-based materials were also explored for degradation applications. The carbon-nitride-immobilised agar-based hybrid aerogel showed excellent photodegradation of dyes, antibiotics and phenol.<sup>300,301</sup> The hybrid aerogel exhibited superior performance to carbon nitride alone or a 60%– $\text{TiO}_2$ -agar hydrogel *via* the synergistic effect of adsorption and photocatalysis. The

hybrid hydrogels can be easily recyclable and the active photocatalyst can be straightforwardly recoverable by heat treatment.<sup>302</sup> The carbon-nitride-impregnated agarose-based beads also prominently exhibit mercury ion adsorption.<sup>303</sup> Further, zeolitic imidazolate framework (ZIF-8) functionalised carbon-nitride-immobilized agar aerogel exhibited superior adsorption of anionic pollutants.<sup>304</sup> This strategy of enhancing the activity by avoiding agglomeration of nanocomposites through immobilization in a biopolymeric network promotes potential applications of nanocomposites with poor dispersability. Furthermore, Patra *et al.* synthesised a bimetallic-functionalised agar-based aerogel as an excellent adsorbent and photocatalyst.<sup>305</sup> The agar@Fe/Pd hybrid nanoparticles exhibited maximum adsorption capacities of  $875 \text{ mg g}^{-1}$  and  $780 \text{ mg g}^{-1}$  for MB and RhB, respectively. The nanocomposite effectively degrading dyes in the presence of  $\text{BH}_4^-$  was attributed to redox reactions triggered by the electrons released from the metal composites. In another study, a laccase-immobilized agarose aerogel was demonstrated for bisphenol degradation.<sup>306</sup> Excellent degradation of endocrine-disrupting chemicals was obtained even with a small concentration of agarose-supported laccase. Moreover, a degradation efficiency of  $>90\%$  was retained even after the 15<sup>th</sup> cycle.

## 6. Carrageenan and other seaweed-derived polysaccharides

Carrageenan, fucoidan, and seaweed-derived cellulose are other biomacromolecules explored for water purification applications. Among them, carrageenan is widely utilised for the preparation of functional polymer gels, beads, membranes and nanocomposites. Carrageenan is a unique linear polysaccharide enriched with sulfate functionalities and has the ability to form polyanions. Structurally, carrageenan is made of alternating 1,3 glycosidic-linked  $\beta$ -D-galactopyranose units and 1,4 glycosidic-linked 3,6-anhydro- $\alpha$ -D-galactopyranose units or 1,4 glycosidic-linked  $\alpha$ -D-galactopyranose units and is commercially obtained by extraction from certain red seaweeds.<sup>307,308</sup> Acrylamide-grafted carrageenan nanocomposites and hydrogels were explored for the adsorption of organic dyes, but a comparatively low adsorption capacity was observed.<sup>309,310</sup> Cellulose/carrageenan hybrids were also explored for organic dye and heavy metal ion adsorption; however, the composites exhibit relatively low adsorption.<sup>311–313</sup> Thus, various carrageenan-based hybrid materials were prepared with GO,<sup>314,315</sup> chitosan,<sup>316</sup> alginate,<sup>317</sup> hydroxyapatite,<sup>318</sup> polydopamine,<sup>319</sup> polyacrylamide,<sup>310</sup>  $\text{TiO}_2$ <sup>319</sup> and zeolites.<sup>320</sup> A GO composite of carrageenan exhibits a high adsorption capacity of  $658.4 \text{ mg g}^{-1}$  for malachite green,<sup>314</sup> whereas a poly(acrylamide-*co*-diallyldimethylammonium chloride)-modified aerogel membrane efficiently separates viscous oil and organic dyes with  $>96\%$  rejection and a flux rate of 40 LMH.<sup>315</sup> The high adsorption capacity and the enhanced separation efficiency are due to multifunctional hydrophobic GO. Similarly, an amine-functionalised  $\text{TiO}_2$ -immobilised carragee-

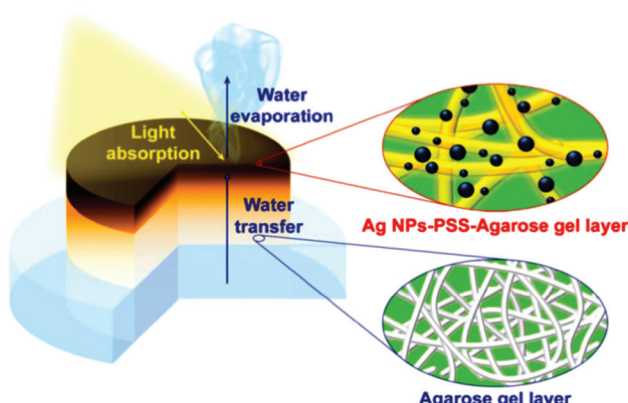


Fig. 12 Schematic representation of agarose-based double-layer hydrogel for solar-assisted water evaporation.<sup>295</sup>

nan hydrogel exhibits a superior adsorption capacity of  $833 \text{ mg g}^{-1}$  for malachite green, attributed to its large surface area, functionality and good affinity.<sup>319</sup> Liang *et al.* demonstrated magnetic  $\text{Fe}_2\text{O}_3$ /chitosan/carrageenan hybrid macro-spheres for the adsorption of dyes and heavy metal ions.<sup>316</sup> The magnetic composite displayed notable adsorption capacities of  $190 \text{ mg g}^{-1}$ ,  $118 \text{ mg g}^{-1}$ ,  $17.9 \text{ mg g}^{-1}$ , and  $10.8 \text{ mg g}^{-1}$  for Congo red, methylene blue,  $\text{Cu}(\text{II})$  and  $\text{Cr}(\text{III})$ , respectively; however, efficient separation was observed in fixed-bed column filtration. Choudhury *et al.* prepared a poly(*N*-vinylpyrrolidone-*co*-acrylic acid)/carrageenan hybrid biocomposite which exhibited high adsorption capacities of  $362.5 \text{ mg g}^{-1}$  and  $398 \text{ mg g}^{-1}$  for Safranine T and brilliant cresyl blue dye, respectively.<sup>321</sup> The hydrophilic  $-\text{COOH}$ ,  $-\text{OH}$  and sulfate group from acrylic acid and carrageenan provide active sites for efficient adsorption through electrostatic interaction. Interestingly, polydopamine-functionalised carrageenan-based aerogel exhibited a high adsorption capacity for heavy metal ions.<sup>318</sup> The terminal amine functionality of polydopamine can form a coordination complex with heavy metal ions and the active sites were further enhanced by the hydroxyl and sulfate groups of carrageenan. The aerogel showed maximum adsorption capacities of  $105 \text{ mg g}^{-1}$ ,  $144.9 \text{ mg g}^{-1}$ ,  $133 \text{ mg g}^{-1}$ ,  $158.7 \text{ mg g}^{-1}$ , and  $128 \text{ mg g}^{-1}$  for  $\text{Cr}(\text{VI})$ ,  $\text{Co}(\text{II})$ ,  $\text{Mn}(\text{II})$ ,  $\text{Cu}(\text{II})$ , and  $\text{Cd}(\text{II})$ , respectively, attributed to high surface area and surface functionalities.

Cellulose is a most abundant, renewable, low-cost biopolymer, mostly extracted from terrestrial plants or biomass. However, cellulose can also be extract from green, red and brown seaweed biomaterials.<sup>322</sup> Cellulose is insoluble in water and most common organic solvents; thus cellulose fibres are mostly explored to prepare functional materials. Hamid and group have functionalised seaweed (*Avicennia marina*) derived cellulose acetate with nano-manganese oxide and utilised it for the adsorption of heavy metal ions.<sup>322</sup> Higher adsorption capacities of  $82 \text{ mg g}^{-1}$  and  $192.8 \text{ mg g}^{-1}$  were obtained for  $\text{Cd}(\text{II})$  and  $\text{Pb}(\text{II})$ , respectively. Further, Yang *et al.* demonstrated the application of a seaweed-derived cellulose-based aerogel for solar-assisted water evaporation.<sup>323</sup> *Ulva* (*Enteromorpha*) *prolifera* derived nanocellulose was crosslinked along with polyvinyl alcohol to form a hydrogel. The self-floating freeze-dried aerogel generated up to  $1.4 \text{ kg m}^{-2} \text{ h}^{-1}$  water vapour under 1-sun illumination. Thus, nanocellulose was utilised as a building block for high-performance functional materials. Another seaweed-derived macromolecule, fucoidan, was also used for the sorption of heavy metal ions.<sup>324–326</sup> Fucoidan is a long polysaccharide enriched with sulfate functional groups. Considerable amounts of  $\text{Pb}(\text{II})$ ,  $\text{Cd}(\text{II})$ ,  $\text{Zn}(\text{II})$  and  $\text{Cu}(\text{II})$  were adsorbed from the fucoidan-based biosorbents, attributed to anionic surface charge and cation exchange capacity.

## 7. Seaweed-derived carbonaceous materials for water purification

Biomass-derived carbonaceous materials have been extensively explored for various applications because they are economical,

environmentally friendly, and can be produced at a large scale. Besides, the valorisation of biomass to produce functional materials is significant over consumption of petroleum-derived products and can be easily commercialized in the near future.<sup>327</sup> Moreover, the biomass-derived carbon materials are biodegradable and evidence shows that biomass-derived carbon can potentially substitute high-cost graphene and graphene oxide derivatives, carbon nanotubes and many metal-based nanocomposites. Additionally, one can design and prepare highly porous, heteroatom-doped and metal-doped graphitic carbonaceous materials by carefully choosing a suitable biomass with additional functionalities of interest.<sup>328,329</sup> They are generally prepared by hydrothermal carbonization or high-temperature pyrolysis or both. In the literature, the majority of biochars reported are obtained from terrestrial lingo-cellulosic feedstocks, which generally yield a carbonaceous product with a C-content of more than 70% with low or negligible nutritive value.<sup>13</sup> It is necessary to induce auxiliary chemicals to obtain carbon with functionalities. For the first time, Zerban and Freeland (1918) prepared biochar from the seaweed *Macrocystis pyrifera* by heating it to about  $800\text{--}900 \text{ }^\circ\text{C}$  for the decolourisation of molasses. However, over the past decade, marine-derived biomaterials have been widely used as carbon precursors for the preparation of multifunctional carbonaceous materials with several advantages. Marine-based biomaterials are inherently enriched with heteroatom-based functionalities and metal ions make them excellent candidates for the preparation of multi-functional carbon.<sup>330</sup> Due to an excessive metal ion content and integrated heteroatom functionalities, they are vastly used for the template-free synthesis of highly porous carbon, while the gases liberated during the pyrolysis create a mesoporous structure, thus avoiding additional reagents for activation.<sup>331</sup> Interestingly, they have also been utilised for the production of graphene/graphitic carbon for various applications, such as energy storage and conversion, as highly efficient adsorbents,<sup>332</sup> and for  $\text{CO}_2$  capture and sensors. However, the present review focuses on the design and development of functional carbonaceous materials for use in efficient water purification.

Various research groups have utilised raw seaweeds to prepare carbonised products due to the presence of significant amounts of metal ions, such as K, Na, Ca, Zn, Mg and Fe, along with heteroatoms such N and P.<sup>32</sup> Additionally, seaweeds are abundant, and thus advantageous in terms of cost and labour for commercial production. Due to the presence of metal ions, hierarchical porous carbons can be obtained by simple acid washing after the pyrolysis.<sup>333</sup> Substantially, the obtained product will also be doped with heteroatoms, which is beneficial for several applications. However, a study showed that the carbonized product obtained from brown-seaweed-based species possesses higher C and H contents and lower S content than red-seaweed-derived biochar.<sup>13</sup> Thus various strategies have been developed to tune the physico-chemical properties of carbonaceous materials, such as porosity, metal ion doping and heteroatom doping, and their efficiencies in adsorbing dyes,<sup>13</sup> heavy metal ions and other pollutants are discussed below and are summarised in Table 2.

**Table 2** Seaweed and seaweed-derived high-performance carbonaceous materials explored for water purification applications

Sl. no.	Biomaterial	Preparation condition	Doping	Surface area	Performance of material	Ref.
01	Kelp biomass	(i) Pyrolysis at 500 °C for 1.5 h; (ii) KOH activation at 600–900 °C, for 2 h followed by acid wash	N-Doped carbon	977–1900 m <sup>2</sup> g <sup>-1</sup>	≈100% degradation of 40 mg L <sup>-1</sup> ofloxacin in 60 min	376
02	<i>Enteromorpha</i> biomass	(i) Pyrolysis at 500 °C for 1.5 h; (ii) KOH activation at 600–900 °C, for 1 h followed by acid wash	Up to 983 m <sup>2</sup> g <sup>-1</sup>	≈100% degradation of paracetamol in 250 s	343	
03	<i>Enteromorpha prolifera</i>	Pyrolysis at 500, 700 or 900 °C for 2 h	N-carbon	—	Selective and powerful nonradical oxidation	328
04	<i>Enteromorpha prolifera</i>	Single-step KOH activation and pyrolysis at 700 °C for 1 h followed by acid wash	Fe/N/C	1262 m <sup>2</sup> g <sup>-1</sup>	Max. adsorption of 910 mg g <sup>-1</sup> for methylene blue	344
05	<i>Enteromorpha</i>	(i) Pyrolysis at 400 °C for 1.5 h; (ii) K <sub>2</sub> CO <sub>3</sub> activation at 500–900 °C, for 2 h followed by acid wash	N-Doped carbon	979–2641 m <sup>2</sup> g <sup>-1</sup>	>95% degradation of 5 mg L <sup>-1</sup> sulfamethoxazole (100 mL) in 90 min	377
06	<i>Enteromorpha prolifera</i>	(i) Functionalisation of seaweed with Fe(OH) <sub>3</sub> ; (ii) pyrolysis at 400 & 800 °C for 2 h	γ-Fe <sub>2</sub> O <sub>3</sub> -Carbon	708–780 m <sup>2</sup> g <sup>-1</sup>	Max. adsorption of 95.23 mg g <sup>-1</sup> for Cr(vi)	378
07	<i>Spirulina</i>	Pyrolysis at 400, 700 or 900 °C for 1.5 h followed by acid wash	N-Doped carbon	370 m <sup>2</sup> g <sup>-1</sup>	Inactivating <i>Escherichia coli</i> via nonradical oxidation	369
08	<i>Ulva fasciata</i> + FeCl <sub>3</sub>	Pyrolysis at 800 °C for 2 h	Fe/FeS-carbon	139.7–376.8 m <sup>2</sup> g <sup>-1</sup>	Max. adsorption of 645 ± 10 mg g <sup>-1</sup> for Pb(ii), 100 mg g <sup>-1</sup> for Cr(vi), 970 mg g <sup>-1</sup> for Congo red, 909 mg g <sup>-1</sup> for crystal violet, 664 mg g <sup>-1</sup> for methyl orange, 402 mg g <sup>-1</sup> for methylene blue.	339
09	<i>Sargassum tenerium</i>	Choline chloride + FeCl <sub>3</sub> /SnCl <sub>3</sub> /ZnCl <sub>3</sub> activation and pyrolysis at 700–900 °C for 2 h	Fe, Zn, Sn-carbon	132–331.7 m <sup>2</sup> g <sup>-1</sup>	Max. adsorption of 75.5 mg g <sup>-1</sup> for fluoride	332
10	<i>Ascophyllum nodosum</i>	KOH-treated hydrothermal carbon prepared at 200 °C for 10 min	Ca-carbon	11.3 m <sup>2</sup> g <sup>-1</sup>	Max. adsorption of 12.3 mg g <sup>-1</sup> for vanadium(v)	379
11	<i>Uva lactuca</i> , <i>Uva reticulata</i> and <i>Caulerpa scalpelliformis</i>	Pyrolysis at 300 or 500 °C for 2 h	—	—	Up to 140.5 mg g <sup>-1</sup> for remazol dyes	330
12	Carageenan	(i) Hydrothermal treatment at 200 °C for 20 h; (ii) KOH activation at 700 °C for 4 h followed by acid wash	—	2800 m <sup>2</sup> g <sup>-1</sup>	Max. adsorption of 459 mg g <sup>-1</sup> for ciprofloxacin	335
13	Chitosan	(i) Hydrothermal treatment at 170–210 °C for 20 h; (ii) pre-carbonized at 300 °C for 30 min; (iii) carbonized at 600–800 °C for 2 h followed by acid wash	—	521–2464 m <sup>2</sup> g <sup>-1</sup>	Max. adsorption of 1599 mg g <sup>-1</sup> for methylene blue	337
14	Chitosan	(i) Freeze drying; (ii) KOH activation at 800 °C for 3 h followed by acid wash	N-Doped carbon	1756 m <sup>2</sup> g <sup>-1</sup>	Removes 20 mg bisphenol A within 10 min	338
15	Chitosan + FeCl <sub>3</sub>	Hydrothermal treatment at 180 °C for 48 h	Fe <sub>2</sub> O <sub>3</sub> -C	59.6 m <sup>2</sup> g <sup>-1</sup>	Max. adsorption of 1.54 mmol g <sup>-1</sup> for Cu(ii), and 2 mmol g <sup>-1</sup> for Cr(vi)	380
16	Chitosan + FeCl <sub>3</sub>	(i) Freeze drying; (ii) KOH activation at 600–800 °C for 2 h	N/Fe <sub>2</sub> O <sub>3</sub> -C	250–600 m <sup>2</sup> g <sup>-1</sup>	Max. adsorption of 263 mg g <sup>-1</sup> mg g <sup>-1</sup> for Cr(vi)	381
17	Calcium alginate	Pyrolysis at 400, 600 or 800 °C for 2 h followed by acid wash	—	112–405 m <sup>2</sup> g <sup>-1</sup>	Max. adsorption of 56 mg g <sup>-1</sup> for Cr(vi)	382
18	Calcium alginate hydrogel	Pyrolysis at 500, 800 or 1000 °C for 2 h	—	221.7–310.8 m <sup>2</sup> g <sup>-1</sup>	Max. adsorption of 7059 mg g <sup>-1</sup> for malachite green, 2390 mg g <sup>-1</sup> for crystal violet, and 6964 mg g <sup>-1</sup> for acid fuchsin	383
19	Sodium alginate + melamine + Co(NO <sub>3</sub> ) <sub>2</sub>	Pyrolysis at 500, 600, 700, 800 or 900 °C for 2 h	N/Co/C	207.1 m <sup>2</sup> g <sup>-1</sup>	Excellent degradation ofponceau, <i>p</i> -nitrophenol and tetracycline, methylene blue in 5 min	371
20	Cellulose/collagen + FeCl <sub>3</sub>	(i) Freeze drying; (ii) pyrolysis 550 or 900 °C for 2 h; and (iii) KOH activation at 800 °C for 2 h	N-Doped carbon	664.3 m <sup>2</sup> g	Max. adsorption of 238.2 mg g <sup>-1</sup> for malachite green and 230.4 mg g <sup>-1</sup> for methylene blue	367

## 7.1 Porous carbonaceous materials

An increase in demand for high-performance sustainable materials has generated tremendous efforts in the areas of design and the synthesis of multifunctional porous carbons. Various techniques, such as hydrothermal treatment followed by high-temperature pyrolysis, acid washing, KOH activation, and template-assisted carbonization have been demonstrated to prepare porous carbonaceous materials. Marine-based biomaterials, especially seaweeds, naturally containing metal ions can help to create a porous structure after calcination assisted by acid washing.<sup>328</sup> However, carbonization of seaweed-derived materials, such as carrageenan, chitosan and alginate, produces highly porous carbon with a remarkable specific surface area compared to the biomass itself. For example, Li *et al.* developed S-doped carbon with a highest surface area of  $4037 \text{ m}^2 \text{ g}^{-1}$  by carbonizing an Fe-carrageenan aerogel followed by KOH activation at  $800^\circ \text{C}$ .<sup>334</sup> An aerogel with a natural porous structure was carbonized up to  $600^\circ \text{C}$  followed by acid washing to remove iron sulfides, yielding a nanoporous structure. Further, KOH activation at  $800^\circ \text{C}$  enhances the porosity to produce a carbonaceous material with the highest specific surface area. In another study, single-step KOH activation of hydrothermally derived carrageenan carbon produced porous carbon materials with a surface area of  $2800 \text{ m}^2 \text{ g}^{-1}$  which is superior to the surface area of commercial activated carbons.<sup>335</sup> The obtained carbon exhibits a maximum adsorption capacity of  $459 \text{ mg g}^{-1}$  for the drug ciprofloxacin, which is several times higher than commercial adsorbents. On the other hand, Liang and group synthesised porous carbon materials with an ultrahigh surface area of  $3532 \text{ m}^2 \text{ g}^{-1}$  by two-step carbonization.<sup>336</sup> Firstly, it was hydrothermally treated at  $200^\circ \text{C}$  for 2 h followed by KOH activation and carbonization which led to the nanoporous structure. Deng *et al.* attempted to prepare high surface area carbon by three-step carbonization using chitosan.<sup>337</sup> Firstly, spherical carbon was prepared by hydrothermal treatment. During the process, acid-catalysed depolymerisation and hydrolysis of gly-

cosidic linkage was followed by condensation polymerisation, resulting in spherical hydrochars. Further, annealing at high temperature results in a hierarchical honeycomb-like structured carbon with a high surface area of  $2464 \text{ m}^2 \text{ g}^{-1}$ . Significantly, the carbon materials displayed an ultrahigh adsorption capacity up to  $1599 \text{ mg g}^{-1}$  for methylene blue. With a similar procedure, alginate yielded a porous carbon with a notable specific surface area of  $749.2 \text{ m}^2 \text{ g}^{-1}$ .<sup>32</sup> Further, Xu *et al.* prepared hierarchical porous structured carbon with a surface area  $1756 \text{ m}^2 \text{ g}^{-1}$  through rapid freezing-assisted carbonization.<sup>338</sup> The material exhibited a remarkable separation efficiency for emerging pollutants such as bisphenol A. Interestingly, the material also exhibited excellent electrical conductivity.

Numerous raw seaweed biomaterials were also carbonized to obtain highly porous carbon. The carbonization of raw biomass is economically significant, since it involves simple pre-treatments such as washing and drying. Our group has developed porous carbon with a notable specific surface area from *Ulva fasciata* and *Sargassum tenerimum* for the adsorption of dyes, heavy metal ions and fluoride from an aqueous medium.<sup>332,339</sup> Recently, we have demonstrated a single-step synthesis of exfoliated carbon nanosheets with a notable surface area of  $700 \text{ m}^2 \text{ g}^{-1}$  using *Salicornia brachiata* (Fig. 13).<sup>340</sup> The inherent salt creates meso- and microporosity; moreover, it assists the exfoliation of carbon materials and avoids the stacking of graphene sheets. Considerably, the carbon displayed remarkable adsorption capacity for heavy metal ions. Similarly, various seaweeds, such as kelp biomass, marine macro-algae, *Enteromorpha prolifera*<sup>341</sup> and *Enteromorpha* biomass were also developed as low-cost precursors for the synthesis of porous carbon and their application in water purification was explored.<sup>342–344</sup>

## 7.2 Heteroatom-doped carbonaceous materials

Heteroatom-doped carbon materials are interesting candidates for energy storage and conversion, water purification, catalysis

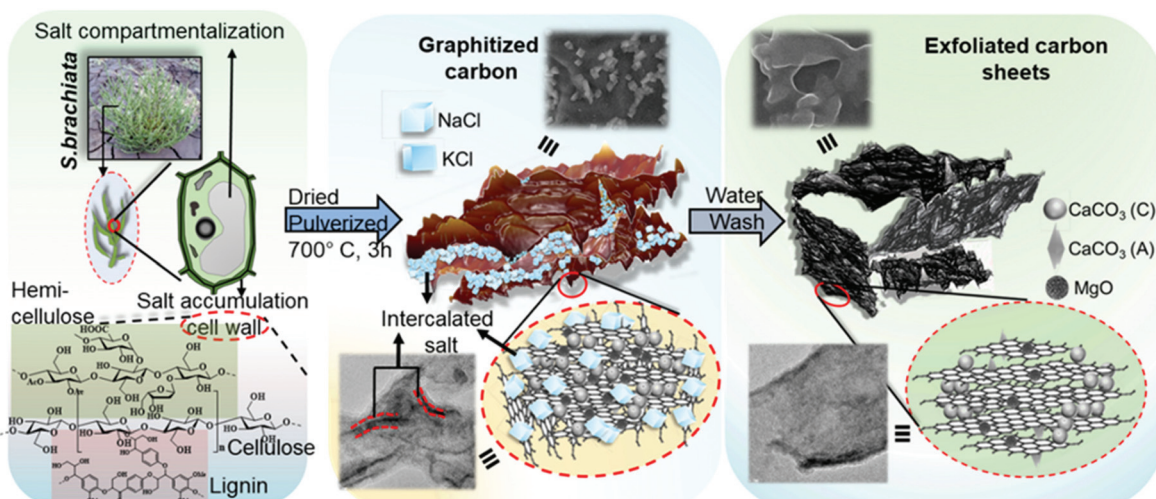


Fig. 13 Schematic representation of the complete process for the fabrication of porous carbon nanosheets from *Salicornia brachiata* biomass.<sup>340</sup>

and many other applications. Heteroatoms such as N, S and P have different atomic orbitals, atomic radii and electronegativity, providing active sites, which greatly enhance the performance of carbon materials for various applications. Thus, remarkable efforts have been made to prepare heteroatom-doped materials using various biomasses, especially those inheriting such functionalities. Marine-derived biomaterials naturally have a large number of amine, phosphate and sulfate functionalities and are excellent candidates to prepare heteroatom-doped carbon without the aid of external chemicals.

For the first time Titirici and group demonstrated the hydrothermal synthesis of nitrogen-containing carbon by using chitosan as a carbon and nitrogen source.<sup>345</sup> Chitosan is naturally rich in nitrogen content (~7 wt%) due to amine and acetamide groups in its structure, making it a promising candidate to prepare carbon materials containing an N-content up to 7–13 wt%.<sup>346</sup> Significantly, annealing of chitosan-based materials provides pyridinic-N, pyrrolic-N and graphitic N-doped carbon materials (Fig. 14).<sup>347</sup> Various attempts were made to prepare N-doped carbon with mesoporosity by high-temperature pyrolysis treatment;<sup>348,349</sup> however, the nitrogen content was comparatively low, which may account for the high-temperature treatment.<sup>350</sup> Interestingly, one can enhance the N-content in carbon materials even under temperature treatment by introducing additional chemicals during the pyrolysis.<sup>351,352</sup> The reports suggested that an increase in the carbonization temperature leads to a substantial decrease in N-content.<sup>353</sup> Nitrogen functionalities of chitosan are known to coordinate with metal ions, suggesting the application of N-doped carbon in water purification applications. Zhong *et al.* explored the adsorption capacity of hydrothermal carbon obtained from chitosan for radioactive elements. The N-doped carbon exhibited a maximum adsorption capacity of 273 mg g<sup>-1</sup> for U(VI).<sup>354,355</sup> Further, the adsorption efficiency was increased up to 408 mg g<sup>-1</sup> by an ion-imprinted technique before hydrothermal treatment which enhanced the selectivity for the target ion.<sup>355</sup>

Later, Shen *et al.* prepared N-doped carbon by hydrothermally treating chitosan from 130 °C to 220 °C and investigated the effect of reaction temperature on tuning the physico-chemical properties of N-doped carbon.<sup>356</sup> Significantly, HTC prepared at 160 °C showed superior adsorption capacity which decreased with an increase in temperature. Notably, incom-

plete carbonization of chitosan was observed when hydrothermally treated at 140 °C. Further, numerous N-doped activated carbons were explored for their adsorption capacity of dyes,<sup>357</sup> phenolic pollutants,<sup>358</sup> heavy metal ions and, also, gaseous pollutants.<sup>356,359</sup> Hameed *et al.* reported the one-step preparation of porous N-doped carbon by impregnating NaOH into the chitosan flakes and then carbonizing them at high temperature followed by an acid wash.<sup>360</sup> The obtained mesoporous activated carbon exhibited a considerable uptake capacity of 143.5 mg g<sup>-1</sup> for methylene blue dye; however, in later studies, KOH-activated N-doped carbon showed an excellent adsorption capacity up to 926 mg g<sup>-1</sup> for malachite green dye.<sup>357</sup> In another study, a graphitic N-doped highly porous carbon aerogel was prepared from chitosan using KOH activation.<sup>338</sup> The material behaved as an excellent adsorbent and catalyst for the degradation of phenolic contaminants. Further, ZnCl<sub>2</sub>-activated carbon was utilised as an efficient adsorbent for various phenolic pollutants and showed a maximum adsorption capacity of 893 mg g<sup>-1</sup> for 2,4-dichlorophenol.<sup>358</sup> The excellent adsorption capacity of these carbon materials is attributed to the increase in surface polarities, enhanced porosity and improved active sites within the carbon framework. Thus, auxiliary chemicals greatly affect the adsorption capacity of carbon. Interestingly, N-doped carbons were also explored as electrocatalysts for H<sub>2</sub>O<sub>2</sub> electrosynthesis for direct application in Fenton-based electrochemical water treatments.<sup>346,351</sup> Although it was not an optimum electrocatalyst, it was demonstrated to be a potentially low-cost and eco-friendly material for water treatment.

Apart from chitosan, various seaweeds, for example, *Ulva fasciata*,<sup>339,361,362</sup> *Spirulina*,<sup>342,363</sup> *Enteromorpha*,<sup>364</sup> *Lessonia nigrescens*,<sup>364</sup> *Meristotheca senegalensis*,<sup>364</sup> and many seaweed-derived biomaterials, such as alginates,<sup>365</sup> carrageenans<sup>366</sup> and collagen<sup>367</sup> were utilised for the preparation of S,N-doped carbon with or without auxiliary chemicals.<sup>368</sup> Chen and group prepared self-N-doped biochar from *Spirulina* residue for non-radical oxidation of *Escherichia coli* bacteria.<sup>369</sup> Huang *et al.* prepared N-doped graphitic carbon material from kelp for peroxy-monosulfate activation.<sup>343</sup> The catalytic degradation process followed the combined reaction of both radical and non-radical pathways of degradation of ciprofloxacin with excellent recyclability and, importantly, independent of metal elements. In both studies, biochar played a versatile role in the activation of peroxy-sulfate *via* an electron transfer regime. On the other hand, carrageenan is a naturally sulfate-rich biopolymer; but the carrageenan-derived carbonaceous materials did not possess a significant amount of sulfur. Thus, intensive research efforts were made to functionalise it with metal nanocomposites.

### 7.3 Metal-doped carbonaceous materials

Carbonaceous materials reinforced with metal nanocomposites show excellent physico-chemical properties for multifunctional applications. In an attempt to prepare a highly porous carbon, our group has demonstrated the scalable production of Fe<sub>3</sub>O<sub>4</sub>/Fe-doped graphene carbon by soft-template-assisted pyrolysis using *Sargassum tenerrimum* (a brown

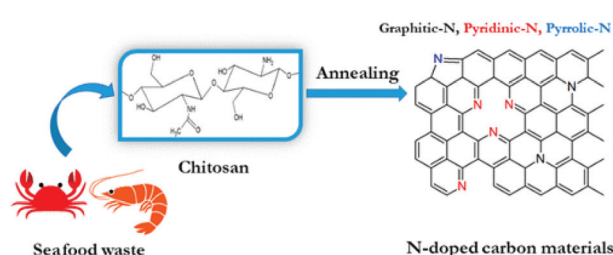


Fig. 14 Pyridinic, pyrrolic and graphitic N-doped carbonaceous materials derived from chitosan.<sup>347</sup>

seaweed).<sup>332</sup> Various metal-based deep eutectic solvents were used as soft templates to prepare porous graphene sheets. The deep eutectic solvent acts as a template to create porous carbon and also acts as source of metal ions to prepare Fe, Zn and Sn doped carbon materials (Fig. 15).<sup>332</sup>

Further, the obtained carbonaceous material exhibited a high surface area and showed a considerable amount of fluoride adsorption from fluoride-rich groundwater attributed to the cationic surface charge.<sup>332</sup> Interestingly, the iron-functionalised carbon exhibits a magnetic property, making it easy to recover from the aqueous medium. We have demonstrated the solvent-free synthesis of graphitic carbon *via* one-step pyrolysis of *Ulva fasciata* in the presence of  $\text{FeCl}_3$  as a templating agent and iron precursor.<sup>339</sup> At elevated temperature, the sulfur-rich biomass has a tendency to convert into sulfides; thus, the carbon materials were doped nanostructured Fe/FeS. The porous graphitic carbon showed superior adsorption efficiency for dyes and heavy metal ions. Further, *Enteromorpha* biomass largely containing iron in its structure was widely explored to prepare Fe-doped carbon. The iron composite in the carbon structure provides active sites for adsorption and also efficiently activates peroxysulfate for radical and nonradical assisted advanced oxidation processes.<sup>328,342</sup> Lin *et al.* prepared non-zero-valent iron-based carbon material ( $\text{Fe}^0/\text{Fe}_3\text{C}$ ) for adsorption and degradation applications by pyrolysing alginate.<sup>376</sup> At low temperature ( $<500\text{ }^\circ\text{C}$ ),  $\text{Fe}_2\text{O}_3/\text{Fe}_3\text{O}_4$  was formed and transformed into  $\text{Fe}_3\text{S}$  when heated to  $>700\text{ }^\circ\text{C}$ . Apart from iron composites, titanium oxide,<sup>366,370</sup> cobalt oxide,<sup>371,374</sup> zinc oxide,<sup>372</sup> magnesium oxide,<sup>373</sup> and silver nanoparticle<sup>375</sup> doped carbonaceous materials were prepared using seaweed or seaweed-derived biomaterials. Generally, metal salts were added as auxiliary chemicals prior to carbonizing, which act as both template and source of metal ion. For example, our group fabricated a  $\text{TiO}_2$ -functionalised carbonaceous photocatalyst using carrageenan for solar-assisted degradation. Interestingly, the surface of the carbon materials is enriched by Brønsted acidic sites caused by sulfur doping, enhancing the photocatalytic activity.<sup>366</sup> The catalyst exhibited complete degradation of dyes within 3–4 h; however, upon using a solar concentrator, the degradation time was reduced to  $<5$  min.

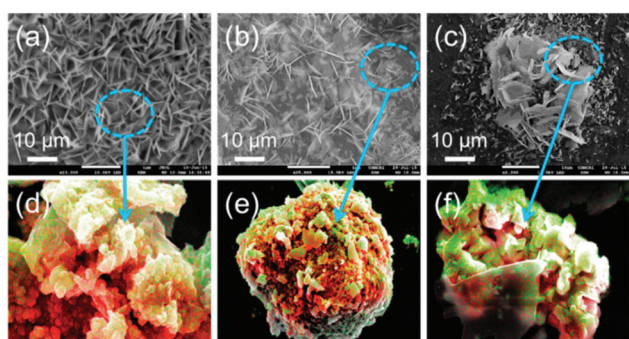


Fig. 15 (a–c) SEM images and (d–f) elemental mapping of graphene-like carbon material obtained by treating *Sargassum tenerrimum* with iron, tin and zinc based DES, respectively.<sup>332</sup>

Further, Zhao *et al.* demonstrated Co/N-doped carbon by chelating cobalt with sodium alginate prior to carbonization for advanced oxidation processes.<sup>371</sup> The bivalent cobalt releases an electron to produce a sulfate radical for degradation of organic molecules in a short interval. Thus, a synergistic combination of an active metal composite with a low-cost functional carbonaceous material shows promising applications in sustainable water purification. Overall, the carbonaceous materials obtained from marine-derived materials are promising candidates for environmental applications because they are economical, biodegradable and can be recyclable.

## 8. Future prospect and conclusions

In sum, marine-derived functional biomaterials are excellent candidates for sustainable water purification applications, attributed to in-built surface functionalities and tunable features. Moreover, they are abundant, renewable, and hence, low-cost and biodegradable. Significantly, huge research development in marine-derived functional materials was accomplished by addressing sustainable water purification. About 70% of the Earth's surface is covered by ocean and this signifies a vast resource of biodiversity. Hence, much attention has been focused on the effective utilisation of marine-derived biomaterials, such as seaweed and chitin, and seaweed-derived macromolecules, such as alginate, agarose, and carrageenan as promising sustainable candidates for water purification. On the other hand, marine-derived materials were also utilised as low-cost feedstocks to prepare valuable multifunctional carbonaceous materials with high porosity, remarkable surface functionality, and metal-functionalised carbon for various applications. Even with the extensive development of highly efficient biosorbents, membranes, and photocatalysts, the materials failed to transfer into commercial application due to complicated implementation and economic feasibility in large-scale operation. Most of the experimental results are predominantly limited to a laboratory scale and fail to be reproduced under flexible environmental conditions. Further, pilot-scale applications of these materials are inadequate for the following reasons:

- Although seaweeds are low-cost, abundant biosorbents, their poor physical and chemical instability causes the leaching of chemical moieties into the aqueous medium, limiting their practical application. Also, the efficient recyclability of seaweeds remains a challenge.
- Chitosans are eco-friendly, non-toxic biodegradable polymers which can potentially substitute conventional synthetic polymers; but their solubility in an acidic medium and non-porous composites limits their large-scale application.
- Besides being hydrophilic, the main drawback with chitosan, alginate and agarose-based materials is their propensity to swell.
- Generally, partial desorption of contaminants was observed due to the enriched surface hetero-functionality; thus, complete regeneration of composites is challenging.

v. Further, chitosan, alginate and agarose-based materials exhibit comparably low mechanical strength, which requires blending with mechanically stable polymers.

By addressing these shortcomings, one can design and significantly develop highly efficient materials for point-of-use sustainable wastewater treatment in the near future. It is notable that the majority of reports are based on empirical approaches and lack molecular-level design. Marine biodiversity includes thousands of seaweed species, exploration of which from various geographical locations could identify additional biomaterials with better structural stability, mechanical strength *etc.* Thus, relevant strategies urgently need to be developed. In addition, the potential of other marine-derived biomaterials and their combinations might be evaluated for water purification applications. On the other hand, carbonaceous materials derived from marine-derived biomaterials exhibit a graphitic nature, high porosity and surface functionality, which could potentially substitute high-cost carbonaceous materials, such as graphene derivatives and carbon nanotubes, for water purification applications. However, very few and a specific class of seaweed-based biopolymers have been explored as sources for biochar and advanced functional 2D carbon materials. Given the diversity of seaweeds, marine invertebrates, and several other carbon resources, it is imperative to broaden the applicability of such abundant resources for the task-specific conversion of functional 2D carbon materials for facile water purification and beyond. Similarly, seaweed-based biopolymer hybrids show excellent performance in solar-assisted water steam generation applications, attributed to the hydrophilicity and high water vapour permeability of the polymers. Although considerable work has been accomplished in the development of marine-derived functional biomaterials for water purification, much work is particularly required to establish their potential application to meet current demand.

## Conflicts of interest

There are no conflicts to declare.

## Acknowledgements

DM thanks RSC Research fund grant (R21-9087288636) for financial support. SKN acknowledge Nanomission Project SR/NM/NT-1073/2016, and Talent Attraction Programme funded by the Community of Madrid (2017-T1/AMB5610).

## Notes and references

- Y. Zhu, C. Romain and C. K. Williams, *Nature*, 2016, **540**, 354–362.
- A. Gandini, T. M. Lacerda, A. J. F. Carvalho and E. Trovatti, *Chem. Rev.*, 2016, **116**, 1637–1669.
- Z. Wang, M. S. Ganewatta and C. Tang, *Prog. Polym. Sci.*, 2020, **101**, 101197.
- D. M. Alonso, J. Q. Bond and J. A. Dumesic, *Green Chem.*, 2010, **12**, 1493–1513.
- R. A. Sheldon, *Green Chem.*, 2014, **16**, 950–963.
- Z. Wang, D. Shen, C. Wu and S. Gu, *Green Chem.*, 2018, **20**, 5031–5057.
- W.-J. Liu, H. Jiang and H.-Q. Yu, *Chem. Rev.*, 2015, **115**, 12251–12285.
- D. Kai, M. J. Tan, P. L. Chee, Y. K. Chua, Y. L. Yap and X. J. Loh, *Green Chem.*, 2016, **18**, 1175–1200.
- A. K. Mohanty, M. Misra and L. T. Drzal, *J. Polym. Environ.*, 2002, **10**, 19–26.
- A. A. Koutinas, A. Vlysidis, D. Pleissner, N. Kopsahelis, I. L. Garcia, I. K. Kookos, S. Papanikolaou, T. H. Kwan and C. S. K. Lin, *Chem. Soc. Rev.*, 2014, **43**, 2587–2627.
- M. Jin, Y. Gai, X. Guo, Y. Hou and R. Zeng, *Mar. Drugs*, 2019, **17**, 656.
- M. H. Centella, A. Arévalo-Gallegos, R. Parra-Saldivar and H. M. N. Iqbal, *J. Cleaner Prod.*, 2017, **168**, 1559–1565.
- D. A. Roberts, N. A. Paul, S. A. Dworjanyn, M. I. Bird and R. de Nys, *Sci. Rep.*, 2015, **5**, 9665.
- Á. M. Mathiesen, *Food and Agriculture Organization of the United Nations*, 2015.
- M. A. Hashim and K. H. Chu, *Chem. Eng. J.*, 2004, **97**, 249–255.
- K. Vijayaraghavan, J. Jegan, K. Palanivelu and M. Velan, *Sep. Purif. Technol.*, 2005, **44**, 53–59.
- G. Pablo, J. S. Gomes-Dias, C. M. Rocha, A. Romaní, G. Garrote and L. Domingues, *Bioresour. Technol.*, 2020, **299**, 122613.
- H. L. Parker, J. R. Dodson, V. L. Budarin, J. H. Clark and A. J. Hunt, *Green Chem.*, 2015, **17**, 2200–2207.
- D. Kühbeck, G. Saidulu, K. R. Reddy and D. D. Díaz, *Green Chem.*, 2012, **14**, 378–392.
- X. Wu, W. Xing, J. Florek, J. Zhou, G. Wang, S. Zhuo, Q. Xue, Z. Yan and F. Kleitz, *J. Mater. Chem. A*, 2014, **2**, 18998–19004.
- M. Y. Song, H. Y. Park, D. S. Yang, D. Bhattacharjya and J. S. Yu, *ChemSusChem*, 2014, **7**, 1755–1763.
- S. K. Nataraj, C.-H. Wang, H.-C. Huang, H.-Y. Du, S.-F. Wang, Y.-C. Chen, L.-C. Chen and K.-H. Chen, *ChemSusChem*, 2012, **5**, 392–395.
- S. Ling, W. Chen, Y. Fan, K. Zheng, K. Jin, H. Yu, M. J. Buehler and D. L. Kaplan, *Prog. Polym. Sci.*, 2018, **85**, 1–56.
- H. M. Manohara, K. Aruchamy, S. Chakraborty, N. Radha, M. R. Nidhi, D. Ghosh, S. K. Nataraj and D. Mondal, *ACS Sustainable Chem. Eng.*, 2019, **7**, 10143–10153.
- V. T. Sharma, H. M. Manohara, S. V. Kamath, D. Mondal and S. K. Nataraj, *Chemosphere*, 2020, **259**, 127421.
- S. Bandehali, H. Sanaeepur, A. E. Amooghin, S. Shirazian and S. Ramakrishna, *Sep. Purif. Technol.*, 2021, **269**, 118731.
- J. R. Dodson, H. L. Parker, A. M. García, A. Hicken, K. Asemave, T. J. Farmer, H. He, J. H. Clark and A. J. Hunt, *Green Chem.*, 2015, **17**, 1951–1965.

28 G. Fadillah, O. A. Saputra and T. A. Saleh, *Trends Environ. Anal. Chem.*, 2020, **26**, e00084.

29 J. R. Dodson, H. L. Parker, A. M. García, A. Hicken, K. Asemave, T. J. Farmer, H. He, J. H. Clark and A. J. Hunt, *Green Chem.*, 2015, **17**, 1951–1965.

30 M. Nasrollahzadeh, M. Sajjadi, S. Iravani and R. S. Varma, *Carbohydr. Polym.*, 2020, 116986.

31 N. Shi, X. Li, T. Fan, H. Zhou, J. Ding, D. Zhang and H. Zhu, *Energy Environ. Sci.*, 2011, **4**, 172–180.

32 D. Mondal, M. Sharma, C.-H. Wang, Y.-C. Lin, H.-C. Huang, A. Saha, S. K. Nataraj and K. Prasad, *Green Chem.*, 2016, **18**, 2819–2826.

33 H. Harrysson, M. Hayes, F. Eimer, N.-G. Carlsson, G. B. Toth and I. Undeland, *J. Appl. Phycol.*, 2018, **30**, 3565–3580.

34 S. Wang, S. Zhao, B. B. Uzoejinwa, A. Zheng, Q. Wang, J. Huang and A. E.-F. Abomohra, *Energy Convers. Manage.*, 2020, **222**, 113253.

35 V. Murphy, H. Hughes and P. McLoughlin, *Water Res.*, 2007, **41**, 731–740.

36 R. H. Vieira and B. Volesky, *Int. Microbiol.*, 2000, **3**, 17–24.

37 C. Ortiz-Calderon, H. C. Silva and D. B. Vásquez, *Biomass volume Estimation and Valorization for energy*, 2017.

38 M. M. Figueira, B. Volesky, V. S. T. Ciminelli and F. A. Roddick, *Water Res.*, 2000, **34**, 196–204.

39 B. Volesky and N. Kuyucak, *Google Patents*, 1988.

40 P. X. Sheng, Y. P. Ting, J. P. Chen and L. Hong, *J. Colloid Interface Sci.*, 2004, **275**, 131–141.

41 P. X. Sheng, Y.-P. Ting and J. P. Chen, *Ind. Eng. Chem. Res.*, 2007, **46**, 2438–2444.

42 V. Murphy, H. Hughes and P. McLoughlin, *Chemosphere*, 2008, **70**, 1128–1134.

43 N. Kuyucak and B. Volesky, *Biotechnol. Bioeng.*, 1989, **33**, 823–831.

44 Y. Suzuki, T. Kametani and T. Maruyama, *Water Res.*, 2005, **39**, 1803–1808.

45 Q. Yu and P. Kaewsarn, *Sep. Sci. Technol.*, 2000, **35**, 689–701.

46 J. T. Matheickal, Q. Yu and G. M. Woodburn, *Water Res.*, 1999, **33**, 335–342.

47 J. T. Matheickal and Q. Yu, *Bioresour. Technol.*, 1999, **69**, 223–229.

48 G. R. de Freitas, M. G. A. Vieira and M. G. C. da Silva, *Ind. Eng. Chem. Res.*, 2018, **57**, 11767–11777.

49 J. Yang and B. Volesky, in *Process Metallurgy*, ed. R. Amils and A. Ballester, Elsevier, 1999, vol. 9, pp. 483–492.

50 H. Omar, A. Abdel-Razek and M. Sayed, *J. Nat. Sci.*, 2010, **8**, 214–221.

51 F. Deniz and A. Karabulut, *Ecol. Eng.*, 2017, **106**, 101–108.

52 A. Essekri, N. Aarab, A. Hsini, Z. Ajmal, M. Laabd, M. El Ouardi, A. Ait Addi, R. Lakhmiri and A. Albourine, *J. Dispersion Sci. Technol.*, 2020, 1–14.

53 M. Kousha, E. Daneshvar, M. S. Sohrabi, M. Jokar and A. Bhatnagar, *Chem. Eng. J.*, 2012, **192**, 67–76.

54 T. A. Davis, B. Volesky and R. H. S. F. Vieira, *Water Res.*, 2000, **34**, 4270–4278.

55 V. J. P. Vilar, C. M. S. Botelho and R. A. R. Boaventura, *Water Res.*, 2006, **40**, 291–302.

56 V. J. Vilar, J. M. Loureiro, C. M. Botelho and R. A. Boaventura, *J. Hazard. Mater.*, 2008, **154**, 1173–1182.

57 R. Angelova, E. Baldikova, K. Pospiskova, Z. Maderova, M. Safarikova and I. Safarik, *J. Cleaner Prod.*, 2016, **137**, 189–194.

58 P. Balaraman, B. Balasubramanian, D. Kaliannan, M. Durai, H. Kamyab, S. Park, S. Chelliapan, C. T. Lee, V. Maluventhen and A. Maruthupandian, *Waste Biomass Valorization*, 2020, **11**, 5255–5271.

59 C. Zhang, P.-L. Show and S.-H. Ho, *Bioresour. Technol.*, 2019, **289**, 121700.

60 C. Zhang, C. Wang, G. Cao, D. Wang and S.-H. Ho, *J. Hazard. Mater.*, 2020, **388**, 121773.

61 D. Aderhold, C. J. Williams and R. G. J. Edyvean, *Bioresour. Technol.*, 1996, **58**, 1–6.

62 B. R. C. Vieira, A. M. A. Pintor, R. A. R. Boaventura, C. M. S. Botelho and S. C. R. Santos, *J. Environ. Manage.*, 2017, **192**, 224–233.

63 S. Z. Rogovina, C. V. Alexanyan and E. V. Prut, *J. Appl. Polym. Sci.*, 2011, **121**, 1850–1859.

64 K. Kurita, *Mar. Biotechnol.*, 2006, **8**, 203.

65 D. Elieh-Ali-Komi and M. R. Hamblin, *Int. J. Adv. Res.*, 2016, **4**, 411–427.

66 P. Sahariah and M. Másson, *Biomacromolecules*, 2017, **18**, 3846–3868.

67 F. Hoppe-Seyler, *Ber. Dtsch. Chem. Ges.*, 1894, **27**, 3329–3331.

68 C. P. Jiménez-Gómez and J. A. Cecilia, *Molecules*, 2020, **25**, 3981.

69 P. Samoila, A. C. Humelnicu, M. Ignat, C. Cojocaru and V. Harabagiu, *Chitin Chitosan: Prop. Appl.*, 2019, 429–460.

70 R. A. Muzzarelli and O. Tubertini, *Talanta*, 1969, **16**, 1571–1577.

71 M. S. Masri, F. W. Reuter and M. Friedman, *J. Appl. Polym. Sci.*, 1974, **18**, 675–681.

72 W. A. Bough and B. WA, *Process Biochem.*, 1976, **11**, 13.

73 M. Rinaudo, *Prog. Polym. Sci.*, 2006, **31**, 603–632.

74 D. Zeng, J. Wu and J. F. Kennedy, *Carbohydr. Polym.*, 2008, **71**, 135–139.

75 F. Renault, B. Sancey, P.-M. Badot and G. Crini, *Eur. Polym. J.*, 2009, **45**, 1337–1348.

76 R. Divakaran and V. N. S. Pillai, *Water Res.*, 2001, **35**, 3904–3908.

77 C. Dong, W. Chen and C. Liu, *Bioresour. Technol.*, 2014, **170**, 239–247.

78 R. Divakaran and V. N. S. Pillai, *J. Appl. Phycol.*, 2002, **14**, 419–422.

79 R. Divakaran and V. N. S. Pillai, *Water Res.*, 2002, **36**, 2414–2418.

80 S. Bratskaya, S. Schwarz and D. Chervonetsky, *Water Res.*, 2004, **38**, 2955–2961.

81 Y.-S. Cheng, Y. Zheng, J. M. Labavitch and J. S. VanderGheynst, *Process Biochem.*, 2011, **46**, 1927–1933.

82 S. Jia, Z. Yang, W. Yang, T. Zhang, S. Zhang, X. Yang, Y. Dong, J. Wu and Y. Wang, *Chem. Eng. J.*, 2016, **283**, 495–503.

83 Z. Yang, H. Yang, Z. Jiang, T. Cai, H. Li, H. Li, A. Li and R. Cheng, *J. Hazard. Mater.*, 2013, **254**, 36–45.

84 L. Ghimici and I. A. Dinu, *Sep. Purif. Technol.*, 2019, **209**, 698–706.

85 B. Liu, X. Chen, H. Zheng, Y. Wang, Y. Sun, C. Zhao and S. Zhang, *Carbohydr. Polym.*, 2018, **181**, 327–336.

86 Z. Yang, H. Li, H. Yan, H. Wu, H. Yang, Q. Wu, H. Li, A. Li and R. Cheng, *J. Hazard. Mater.*, 2014, **276**, 480–488.

87 P. Loganathan, M. Gradielski, H. Bustamante and S. Vigneswaran, *Environ. Sci.: Water Res. Technol.*, 2020, **6**, 45–61.

88 C. Kaseamchochoung, P. Lertsutthiwong and C. Phalakornkhule, *Water Environ. Res.*, 2006, **78**, 2210–2216.

89 H. Karimi-Maleh, A. Ayati, R. Davoodi, B. Tanhaei, F. Karimi, S. Malekmohammadi, Y. Orooji, L. Fu and M. Sillanpää, *J. Cleaner Prod.*, 2021, 125880.

90 W. W. Ngah, L. Teong and M. M. Hanafiah, *Carbohydr. Polym.*, 2011, **83**, 1446–1456.

91 S. Mincke, T. G. Asere, I. Verheyen, K. Folens, F. Vanden Bussche, L. Lapeire, K. Verbeken, P. Van Der Voort, D. A. Tessema, F. Fufa, G. Du Laing and C. V. Stevens, *Green Chem.*, 2019, **21**, 2295–2306.

92 U. Baruah, A. Konwar and D. Chowdhury, *Nanoscale*, 2016, **8**, 8542–8546.

93 W.-Z. Qiu, Q.-Z. Zhong, Y. Du, Y. Lv and Z.-K. Xu, *Green Chem.*, 2016, **18**, 6205–6208.

94 X. Shen, J. L. Shamshina, P. Berton, G. Gurau and R. D. Rogers, *Green Chem.*, 2016, **18**, 53–75.

95 G. Gibbs, J. M. Tobin and E. Guibal, *J. Appl. Polym. Sci.*, 2003, **90**, 1073–1080.

96 I. O. Saheed, O. W. Da and F. B. M. Suah, *J. Hazard. Mater.*, 2020, 124889.

97 K. Z. Elwakeel, M. A. Abd El-Ghaffar, S. M. El-kousy and H. G. El-Shorbagy, *Chem. Eng. J.*, 2012, **203**, 458–468.

98 X. Jiang, Y. Sun, L. Liu, S. Wang and X. Tian, *Chem. Eng. J.*, 2014, **235**, 151–157.

99 V. Singh, A. K. Sharma, D. N. Tripathi and R. Sanghi, *J. Hazard. Mater.*, 2009, **161**, 955–966.

100 Y. Yan, B. Xiang, Y. Li and Q. Jia, *J. Appl. Polym. Sci.*, 2013, **130**, 4090–4098.

101 M. Sadeghi-Kiakhani, M. Arami and K. Gharanjig, *J. Appl. Polym. Sci.*, 2013, **127**, 2607–2619.

102 G. Z. Kyzas, D. N. Bikaris and D. A. Lambropoulou, *J. Mol. Liq.*, 2017, **230**, 1–5.

103 S. Sharma and N. Rajesh, *J. Environ. Chem. Eng.*, 2017, **5**, 1927–1935.

104 Y. Jiang, B. Liu, J. Xu, K. Pan, H. Hou, J. Hu and J. Yang, *Carbohydr. Polym.*, 2018, **182**, 106–114.

105 M. Salzano de Luna, C. Ascione, C. Santillo, L. Verdolotti, M. Lavorgna, G. G. Buonocore, R. Castaldo, G. Filippone, H. Xia and L. Ambrosio, *Carbohydr. Polym.*, 2019, **211**, 195–203.

106 Z. Li, X. Song, S. Cui, Y. Jiao and C. Zhou, *RSC Adv.*, 2018, **8**, 8338–8348.

107 L. Fan, C. Luo, X. Li, F. Lu, H. Qiu and M. Sun, *J. Hazard. Mater.*, 2012, **215–216**, 272–279.

108 A. ZabihiSahebi, S. Koushkbaghi, M. Pishnamazi, A. Askari, R. Khosravi and M. Irani, *Int. J. Biol. Macromol.*, 2019, **140**, 1296–1304.

109 H. Mahmoodian, O. Moradi, B. Shariatzadeha, T. A. Salehf, I. Tyagi, A. Maity, M. Asif and V. K. Gupta, *J. Mol. Liq.*, 2015, **202**, 189–198.

110 Q. Liu, J. Shi, J. Sun, T. Wang, L. Zeng and G. Jiang, *Angew. Chem.*, 2011, **123**, 6035–6039.

111 K. Thakur and B. Kandasubramanian, *J. Chem. Eng. Data*, 2019, **64**, 833–867.

112 D. C. d. S. Alves, B. Healy, T. Yu and C. B. Breslin, *Materials*, 2021, **14**, 3655.

113 A. O. Salawudeen, B. S. Tawabini, A. M. Al-Shaibani and T. A. Saleh, *Environ. Nanotechnol. Monit. Manag.*, 2020, **13**, 100288.

114 G. Fadillah, W. P. Wicaksono, I. Fatimah and T. A. Saleh, *Microchem. J.*, 2020, **159**, 105353.

115 A. M. Alansi, T. F. Qahtan and T. A. Saleh, *Adv. Mater. Interfaces*, 2021, **8**, 2001463.

116 A. Q. Al-Gamal, W. S. Falath and T. A. Saleh, *J. Mol. Liq.*, 2021, **323**, 114922.

117 B. O. Abdulla, E. Ahmed, H. Al Abdulgader, F. Alghunaimi and T. A. Saleh, *J. Mol. Liq.*, 2021, **325**, 115057.

118 I. Ali and T. A. Saleh, *Appl. Catal. A*, 2020, **598**, 117542.

119 T. A. Saleh, *Trends Environ. Anal. Chem.*, 2020, **25**, e00080.

120 K. Haruna and T. A. Saleh, *J. Environ. Chem. Eng.*, 2021, **9**, 104967.

121 T. A. Saleh and S. A. Al-Hammadi, *Chem. Eng. J.*, 2021, **406**, 125167.

122 T. A. Saleh, K. Haruna and A.-R. I. Mohammed, *J. Mol. Liq.*, 2021, **325**, 115060.

123 Y. Chen, L. Chen, H. Bai and L. Li, *J. Mater. Chem. A*, 2013, **1**, 1992–2001.

124 M. A. Kamal, S. Bibi, S. W. Bokhari, A. H. Siddique and T. Yasin, *React. Funct. Polym.*, 2017, **110**, 21–29.

125 P. Banerjee, S. R. Barman, A. Mukhopadhyay and P. Das, *Chem. Eng. Res. Des.*, 2017, **117**, 43–56.

126 M. Salzano de Luna, C. Ascione, C. Santillo, L. Verdolotti, M. Lavorgna, G. G. Buonocore, R. Castaldo, G. Filippone, H. Xia and L. Ambrosio, *Carbohydr. Polym.*, 2019, **211**, 195–203.

127 Z. Yi, L. Huajie, L. Mingchun and X. Meihua, *J. Mol. Struct.*, 2020, **1209**, 127973.

128 L. Fan, C. Luo, M. Sun, X. Li, F. Lu and H. Qiu, *Bioresour. Technol.*, 2012, **114**, 703–706.

129 L. Fan, C. Luo, M. Sun, H. Qiu and X. Li, *Colloids Surf., B*, 2013, **103**, 601–607.

130 L. Li, L. Fan, C. Luo, H. Duan and X. Wang, *RSC Adv.*, 2014, **4**, 24679–24685.

131 Y. Jiang, J.-L. Gong, G.-M. Zeng, X.-M. Ou, Y.-N. Chang, C.-H. Deng, J. Zhang, H.-Y. Liu and S.-Y. Huang, *Int. J. Biol. Macromol.*, 2016, **82**, 702–710.

132 B. Ramalingam, M. M. R. Khan, B. Mondal, A. B. Mandal and S. K. Das, *ACS Sustainable Chem. Eng.*, 2015, **3**, 2291–2302.

133 M. Hui, P. Shengyan, H. Yaqi, Z. Rongxin, Z. Anatoly and C. Wei, *Chem. Eng. J.*, 2018, **345**, 556–565.

134 N. Singh, S. Riyajuddin, K. Ghosh, S. K. Mehta and A. Dan, *ACS Appl. Nano Mater.*, 2019, **2**, 7379–7392.

135 H. Tu, Y. Yu, J. Chen, X. Shi, J. Zhou, H. Deng and Y. Du, *Polym. Chem.*, 2017, **8**, 2913–2921.

136 D.-M. Guo, Q.-D. An, Z.-Y. Xiao, S.-R. Zhai and D.-J. Yang, *Carbohydr. Polym.*, 2018, **202**, 306–314.

137 C. Lei, F. Wen, J. Chen, W. Chen, Y. Huang and B. Wang, *Polymer*, 2021, **213**, 123316.

138 W. Zhu, X. Jiang, F. Liu, F. You and C. Yao, *Polymers*, 2020, **12**, 2169.

139 Saakshy, K. Singh, A. B. Gupta and A. K. Sharma, *J. Cleaner Prod.*, 2016, **112**, 1227–1240.

140 P. Yu, H.-Q. Wang, R.-Y. Bao, Z. Liu, W. Yang, B.-H. Xie and M.-B. Yang, *ACS Sustainable Chem. Eng.*, 2017, **5**, 1557–1566.

141 M. H. Mruthunjayappa, V. T. Sharma, K. Dharmalingam, S. K. Nataraj and D. Mondal, *ACS Appl. Bio Mater.*, 2020, **3**, 5233–5243.

142 D. Ma, H. Yi, C. Lai, X. Liu, X. Huo, Z. An, L. Li, Y. Fu, B. Li and M. Zhang, *Chemosphere*, 2021, 130104.

143 S. Mozia, *Sep. Purif. Technol.*, 2010, **73**, 71–91.

144 M. A. M. Adnan, B. L. Phoon and N. M. Julkapli, *J. Cleaner Prod.*, 2020, **261**, 121190.

145 P. Demircivi and E. B. Simsek, *Water Sci. Technol.*, 2018, **78**, 487–495.

146 G. Xiao, H. Su and T. Tan, *J. Hazard. Mater.*, 2015, **283**, 888–896.

147 P. Wu, H. Peng, Y. Wu, L. Li, X. Hao, B. Peng, G. Meng, J. Wu and Z. Liu, *J. Electron. Sci. Technol.*, 2020, **18**, 100019.

148 S. Preethi, K. Abarna, M. Nithyasri, P. Kishore, K. Deepika, R. Ranjithkumar, V. Bhuvaneshwari and D. Bharathi, *Int. J. Biol. Macromol.*, 2020, **164**, 2779–2787.

149 A. M. Saad, M. R. Abukhadra, S. Abdel-Kader Ahmed, A. M. Elzanaty, A. H. Mady, M. A. Betiha, J. J. Shim and A. M. Rabie, *J. Environ. Manage.*, 2020, **258**, 110043.

150 Z. Zainal, L. K. Hui, M. Z. Hussein and A. H. Abdullah, *J. Hazard. Mater.*, 2009, **164**, 138–145.

151 A. Balakrishnan, S. Appunni and K. Gopalram, *Int. J. Biol. Macromol.*, 2020, **161**, 282–291.

152 X. Wang, J. Song, J. Huang, J. Zhang, X. Wang, R. Ma, J. Wang and J. Zhao, *Appl. Surf. Sci.*, 2016, **390**, 190–201.

153 S. Cheng, C. Zhang, J. Li, X. Pan, X. Zhai, Y. Jiao, Y. Li, W. Dong and X. Qi, *Carbohydr. Polym.*, 2021, **262**, 117951.

154 M. R. Abukhadra, A. Adlii and B. M. Bakry, *Int. J. Biol. Macromol.*, 2019, **126**, 402–413.

155 A. A. P. Mansur, H. S. Mansur, F. P. Ramanery, L. C. Oliveira and P. P. Souza, *Appl. Catal., B*, 2014, **158–159**, 269–279.

156 K.-Y. A. Lin, J.-T. Lin and H. Yang, *Carbohydr. Polym.*, 2017, **173**, 412–421.

157 T. Oe, H. Koide, H. Hirokawa and K. Okukawa, *Desalination*, 1996, **106**, 107–113.

158 R. Zhang, Y. Liu, M. He, Y. Su, X. Zhao, M. Elimelech and Z. Jiang, *Chem. Soc. Rev.*, 2016, **45**, 5888–5924.

159 M. Beppu, R. Vieira, C. Aimoli and C. Santana, *J. Membr. Sci.*, 2007, **301**, 126–130.

160 M. M. Beppu, R. S. Vieira, C. G. Aimoli and C. C. Santana, *J. Membr. Sci.*, 2007, **301**, 126–130.

161 A. Mochizuki, Y. Sato, H. Ogawara and S. Yamashita, *J. Appl. Polym. Sci.*, 1989, **37**, 3375–3384.

162 X. P. Wang, Z. Q. Shen and F. Y. Zhang, *J. Appl. Polym. Sci.*, 1998, **69**, 2035–2041.

163 G. Qunhui, H. Ohya and Y. Negishi, *J. Membr. Sci.*, 1995, **98**, 223–232.

164 D. Anjali Devi, B. Smitha, S. Sridhar and T. M. Aminabhavi, *J. Membr. Sci.*, 2005, **262**, 91–99.

165 W. Won, X. Feng and D. Lawless, *Sep. Purif. Technol.*, 2003, **31**, 129–140.

166 M. Gierszewska and J. Ostrowska-Czubenko, *Carbohydr. Polym.*, 2016, **153**, 501–511.

167 S. Liu, Z. Wang and P. Song, *ACS Sustainable Chem. Eng.*, 2018, **6**, 4253–4263.

168 J. Wang, X. Gao, J. Wang, Y. Wei, Z. Li and C. Gao, *ACS Appl. Mater. Interfaces*, 2015, **7**, 4381–4389.

169 Y. Song, Q. Hu, T. Li, Y. Sun, X. Chen and J. Fan, *Chem. Eng. J.*, 2018, **352**, 163–172.

170 J. Xu, X. Feng and C. Gao, *J. Membr. Sci.*, 2011, **370**, 116–123.

171 R. Kumar, A. M. Isloor and A. F. Ismail, *Desalination*, 2014, **350**, 102–108.

172 A. Giwa, N. Akther, V. Dufour and S. W. Hasan, *RSC Adv.*, 2016, **6**, 8134–8163.

173 M. Halakarni, A. Mahto, K. Aruchamy, D. Mondal and S. K. Nataraj, *Chem. Eng. J.*, 2021, **417**, 127911.

174 N. R. Maalige, K. Aruchamy, V. Polishetti, M. Halakarni, A. Mahto, D. Mondal and S. K. Nataraj, *Carbohydr. Polym.*, 2021, **254**, 117297.

175 K. H. Vardhan, P. S. Kumar and R. C. Panda, *J. Mol. Liq.*, 2019, **290**, 111197.

176 X. Liu, Q. Hu, Z. Fang, X. Zhang and B. Zhang, *Langmuir*, 2009, **25**, 3–8.

177 T. Jin, T. Liu, E. Lam and A. Moores, *Nanoscale Horiz.*, 2021, **6**, 505–542.

178 M. Nasrollahzadeh, M. Sajjadi, S. Iravani and R. S. Varma, *Carbohydr. Polym.*, 2021, **251**, 116986.

179 G. Crini, *Prog. Polym. Sci.*, 2005, **30**, 38–70.

180 M. J. Ahmed, B. H. Hameed and E. H. Hummadi, *Carbohydr. Polym.*, 2020, **247**, 116690.

181 V. K. Thakur and S. I. Voicu, *Carbohydr. Polym.*, 2016, **146**, 148–165.

182 K. H. Prashanth and R. Tharanathan, *Trends Food Sci. Technol.*, 2007, **18**, 117–131.

183 M. J. Zohuriaan-Mehr, *Iran. Polym. J.*, 2005, **14**, 235–265.

184 J. Roosen and K. Binnemans, *J. Mater. Chem. A*, 2014, **2**, 1530–1540.

185 D. Zhang, L. Wang, H. Zeng, B. Rhimi and C. Wang, *Environ. Sci. Nano*, 2020, **7**, 793–802.

186 J. Wang and C. Chen, *Bioresour. Technol.*, 2014, **160**, 129–141.

187 G. Jing, L. Wang, H. Yu, W. A. Amer and L. Zhang, *Colloids Surf., A*, 2013, **416**, 86–94.

188 J. Roosen, J. Spooren and K. Binnemans, *J. Mater. Chem. A*, 2014, **2**, 19415–19426.

189 Y. Zhang, M. Yin, L. Li, B. Fan, Y. Liu, R. Li, X. Ren, T.-S. Huang and I. S. Kim, *Carbohydr. Polym.*, 2020, **243**, 116461.

190 S. Mallakpour, E. Azadi and C. M. Hussain, *New J. Chem.*, 2021, **45**, 3756–3777.

191 M. Ahmed, B. Hameed and E. Hummadi, *Carbohydr. Polym.*, 2020, 116690.

192 G. Yu, Y. Lu, J. Guo, M. Patel, A. Bafana, X. Wang, B. Qiu, C. Jeffries, S. Wei and Z. Guo, *Adv. Compos. Hybrid Mater.*, 2018, **1**, 56–78.

193 M. J. Sweetman, S. May, N. Mebberson, P. Pendleton, K. Vasilev, S. E. Plush and J. D. Hayball, *C*, 2017, **3**, 18.

194 M. U. Sankar, S. Aigal, S. M. Maliyekkal, A. Chaudhary, Anshup, A. A. Kumar, K. Chaudhari and T. Pradeep, *Proc. Natl. Acad. Sci. U. S. A.*, 2013, **110**, 8459–8464.

195 A. A. Kumar, A. Som, P. Longo, C. Sudhakar, R. G. Bhui, S. S. Gupta, Anshup, M. U. Sankar, A. Chaudhary, R. Kumar and T. Pradeep, *Adv. Mater.*, 2017, **29**, 1604260.

196 Z. Wan, W. Chen, C. Liu, Y. Liu and C. Dong, *J. Colloid Interface Sci.*, 2015, **443**, 115–124.

197 Z. Marková, K. Šišková, J. Filip, K. Šafářová, R. Prucek, A. Panáček, M. Kolář and R. Zbořil, *Green Chem.*, 2012, **14**, 2550–2558.

198 Z. Yu, X. Zhang and Y. Huang, *Ind. Eng. Chem. Res.*, 2013, **52**, 11956–11966.

199 J. Li, B. Jiang, Y. Liu, C. Qiu, J. Hu, G. Qian, W. Guo and H. H. Ngo, *J. Cleaner Prod.*, 2017, **158**, 51–58.

200 G. L. Rorrer, T. Y. Hsien and J. D. Way, *Ind. Eng. Chem. Res.*, 1993, **32**, 2170–2178.

201 P. E. Hande, S. Kamble, A. B. Samui and P. S. Kulkarni, *Ind. Eng. Chem. Res.*, 2016, **55**, 3668–3678.

202 D. Kong, N. Wang, N. Qiao, Q. Wang, Z. Wang, Z. Zhou and Z. Ren, *ACS Sustainable Chem. Eng.*, 2017, **5**, 7401–7409.

203 Q. Wang, X. Liu, M. Zhang, Z. Wang, Z. Zhou and Z. Ren, *Ind. Eng. Chem. Res.*, 2019, **58**, 6670–6678.

204 H. N. Doan, P. P. Vo, A. Baggio, M. Negoro, K. Kinashi, Y. Fuse, W. Sakai and N. Tsutsumi, *ACS Appl. Poly. Mater.*, 2021.

205 J. Ma, X. Fu, W. Xia, R. Zhang, K. Fu, G. Wu, B. Jia, S. Li and J. Li, *J. Hazard. Mater.*, 2021, 126529.

206 A. Pinotti, A. Bevilacqua and N. Zaritzky, *J. Surfactants Deterg.*, 2001, **4**, 57–63.

207 S. Bratskaya, V. Avramenko, S. Schwarz and I. Philippova, *Colloids Surf., A*, 2006, **275**, 168–176.

208 R. Yang, H. Li, M. Huang, H. Yang and A. Li, *Water Res.*, 2016, **95**, 59–89.

209 J. Liu, P. Li, L. Chen, Y. Feng, W. He, X. Yan and X. Lü, *Surf. Coat. Technol.*, 2016, **307**, 171–176.

210 J. P. Chaudhary, N. Vadodariya, S. K. Nataraj and R. Meena, *ACS Appl. Mater. Interfaces*, 2015, **7**, 24957–24962.

211 (a) R. Meena, N. D. Sanandiya, J. P. Chaudhary, D. Mondal and S. K. Nataraj, 2015056273A4, 2015; (b) J. P. Chaudhary, S. K. Nataraj, A. Gogda and R. Meena, *Green Chem.*, 2014, **16**, 4552–4558.

212 N. Cao, Q. Lyu, J. Li, Y. Wang, B. Yang, S. Szunerits and R. Boukherroub, *Chem. Eng. J.*, 2017, **326**, 17–28.

213 W. Zhou, Y. Fang, P. Li, L. Yan, X. Fan, Z. Wang, W. Zhang and H. Liu, *ACS Sustainable Chem. Eng.*, 2019, **7**, 15463–15470.

214 H. Zhang, Y. Li, R. Shi, L. Chen and M. Fan, *Carbohydr. Polym.*, 2018, **200**, 611–615.

215 J. Hu, J. Zhu, S. Ge, C. Jiang, T. Guo, T. Peng, T. Huang and L. Xie, *Surf. Coat. Technol.*, 2020, **385**, 125361.

216 L. Yi, J. Yang, X. Fang, Y. Xia, L. Zhao, H. Wu and S. Guo, *J. Hazard. Mater.*, 2020, **385**, 121507.

217 M. Wang, Y. Ma, Y. Sun, S. Y. Hong, S. K. Lee, B. Yoon, L. Chen, L. Ci, J.-D. Nam, X. Chen and J. Suhr, *Sci. Rep.*, 2017, **7**, 18054.

218 X. Zhou, F. Zhao, Y. Guo, B. Rosenberger and G. Yu, *Sci. Adv.*, 2019, **5**, eaaw5484.

219 T. Xu, Y. Xu, J. Wang, H. Lu, W. Liu and J. Wang, *Chem. Eng. J.*, 2021, **415**, 128893.

220 F. Wang, D. Wei, Y. Li, T. Chen, P. Mu, H. Sun, Z. Zhu, W. Liang and A. Li, *J. Mater. Chem. A*, 2019, **7**, 18311–18317.

221 X.-Y. Wang, J. Xue, C. Ma, T. He, H. Qian, B. Wang, J. Liu and Y. Lu, *J. Mater. Chem. A*, 2019, **7**, 16696–16703.

222 S. Zhang, F. Lu, L. Tao, N. Liu, C. Gao, L. Feng and Y. Wei, *ACS Appl. Mater. Interfaces*, 2013, **5**, 11971–11976.

223 M. Zhang, W. Xu, M. Li, J. Li, P. Wang and Z. Wang, *J. Bionic Eng.*, 2021, **18**, 30–39.

224 F. Yu, Z. Chen, Z. Guo, M. S. Irshad, L. Yu, J. Qian, T. Mei and X. Wang, *ACS Sustainable Chem. Eng.*, 2020, **8**, 7139–7149.

225 X. Wang, Z. Li, Y. Wu, H. Guo, X. Zhang, Y. Yang, H. Mu and J. Duan, *ACS Appl. Mater. Interfaces*, 2021, **13**, 10902–10915.

226 M. S. Irshad, X. Wang, M. S. Abbasi, N. Arshad, Z. Chen, Z. Guo, L. Yu, J. Qian, J. You and T. Mei, *ACS Sustainable Chem. Eng.*, 2021, **9**, 3887–3900.

227 B. Rehm and S. Valla, *Appl. Microbiol. Biotechnol.*, 1997, **48**, 281–288.

228 I. P. S. Fernando, W. Lee, E. J. Han and G. Ahn, *Chem. Eng. J.*, 2020, **391**, 123823.

229 S. D. Bhat and T. M. Aminabhavi, *Sep. Purif. Rev.*, 2007, **36**, 203–229.

230 J.-S. Yang, Y.-J. Xie and W. He, *Carbohydr. Polym.*, 2011, **84**, 33–39.

231 Z. Aksu, G. Egretli and T. Kutsal, *J. Environ. Sci. Health, Part A: Toxic/Hazard. Subst. Environ. Eng.*, 1999, **34**, 295–316.

232 Y. Sag, M. Nourbakhsh, Z. Aksu and T. Kutsal, *Process Biochem.*, 1995, **30**, 175–181.

233 J. H. Min and J. G. Hering, *Water Res.*, 1998, **32**, 1544–1552.

234 K. SAITO, T. MURATA and T. MORI, *Int. J. Food Sci. Technol.*, 1994, **29**, 715–719.

235 G. Annadurai, R.-S. Juang and D.-J. Lee, *Adv. Environ. Res.*, 2002, **6**, 191–198.

236 R. Aravindhan, N. N. Fathima, J. R. Rao and B. U. Nair, *Colloids Surf., A*, 2007, **299**, 232–238.

237 E. Prouzet, Z. Khani, M. Bertrand, M. Tokumoto, V. Guyot-Ferreol and J.-F. Tranchant, *Microporous Mesoporous Mater.*, 2006, **96**, 369–375.

238 C. Wang, H. Liu, Q. Gao, X. Liu and Z. Tong, *Carbohydr. Polym.*, 2008, **71**, 476–480.

239 A. Ely, M. Baudu, M. O. S. A. O. Kankou and J.-P. Basly, *Chem. Eng. J.*, 2011, **178**, 168–174.

240 S. Peretz, D. F. Anghel, E. Vasilescu, M. Florea-Spiroiu, C. Stoian and G. Zgherean, *Polym. Bull.*, 2015, **72**, 3169–3182.

241 S. Partap, A. Muthutantri, I. U. Rehman, G. R. Davis and J. A. Darr, *J. Mater. Sci.*, 2007, **42**, 3502–3507.

242 S. Pashaei-Fakhri, S. J. Peighambarioust, R. Foroutan, N. Arsalani and B. Ramavandi, *Chemosphere*, 2021, **270**, 129419.

243 T. Hu, Q. Liu, T. Gao, K. Dong, G. Wei and J. Yao, *ACS Omega*, 2018, **3**, 7523–7531.

244 J. Fan, Z. Shi, M. Lian, H. Li and J. Yin, *J. Mater. Chem. A*, 2013, **1**, 7433–7443.

245 W. Wang, Y. Zhao, H. Bai, T. Zhang, V. Ibarra-Galvan and S. Song, *Carbohydr. Polym.*, 2018, **198**, 518–528.

246 Z.-j. Shao, X.-l. Huang, F. Yang, W.-f. Zhao, X.-z. Zhou and C.-s. Zhao, *Carbohydr. Polym.*, 2018, **187**, 85–93.

247 Y. Feng, H. Wang, J. Xu, X. Du, X. Cheng, Z. Du and H. Wang, *J. Hazard. Mater.*, 2021, **416**, 125777.

248 S. Thakur, S. Pandey and O. A. Arotiba, *Carbohydr. Polym.*, 2016, **153**, 34–46.

249 E. Makhado, S. Pandey, K. D. Modibane, M. Kang and M. J. Hato, *Int. J. Biol. Macromol.*, 2020, **162**, 60–73.

250 K. Sui, Y. Li, R. Liu, Y. Zhang, X. Zhao, H. Liang and Y. Xia, *Carbohydr. Polym.*, 2012, **90**, 399–406.

251 A. F. Hassan, A. M. Abdel-Mohsen and M. M. G. Fouda, *Carbohydr. Polym.*, 2014, **102**, 192–198.

252 L. Gan, H. Li, L. Chen, L. Xu, J. Liu, A. Geng, C. Mei and S. Shang, *Colloid Polym. Sci.*, 2018, **296**, 607–615.

253 Q. Li, Y. Li, X. Ma, Q. Du, K. Sui, D. Wang, C. Wang, H. Li and Y. Xia, *Chem. Eng. J.*, 2017, **316**, 623–630.

254 S. Lin, R. Huang, Y. Cheng, J. Liu, B. L. Lau and M. R. Wiesner, *Water Res.*, 2013, **47**, 3959–3965.

255 X. Li, H. Lu, Y. Zhang, F. He, L. Jing and X. He, *Appl. Surf. Sci.*, 2016, **389**, 567–577.

256 V. S. Munagapati and D.-S. Kim, *Ecotoxicol. Environ. Saf.*, 2017, **141**, 226–234.

257 Y. Kong, Y. Zhuang, K. Han and B. Shi, *Colloids Surf., A*, 2020, **588**, 124360.

258 S. Sarkar, S. Chakraborty and C. Bhattacharjee, *Ecotoxicol. Environ. Saf.*, 2015, **121**, 263–270.

259 S. K. Papageorgiou, F. K. Katsaros, E. P. Favvas, G. E. Romanos, C. P. Athanasekou, K. G. Beltsios, O. I. Tzialla and P. Falaras, *Water Res.*, 2012, **46**, 1858–1872.

260 S. K. Mohamed, S. H. Hegazy, N. A. Abdelwahab and A. M. Ramadan, *Int. J. Biol. Macromol.*, 2018, **108**, 1185–1198.

261 D. Hao, Q. Huang, W. Wei, X. Bai and B.-J. Ni, *J. Cleaner Prod.*, 2021, **314**, 128033.

262 D. Qian, L. Bai, Y.-S. Wang, F. Song, X.-L. Wang and Y.-Z. Wang, *Ind. Eng. Chem. Res.*, 2019, **58**, 13133–13144.

263 K. Wanchai, *Key Eng. Mater.*, 2017, **751**, 689–694.

264 I. Hasan, C. Shekhar, I. I. B. Sharfan, R. A. Khan and A. Alsalme, *ACS Omega*, 2020, **5**, 32011–32022.

265 L. Li, Y. Fang, R. Vreeker, I. Appelqvist and E. Mendes, *Biomacromolecules*, 2007, **8**, 464–468.

266 S. Peretz and O. Cintez, *Colloids Surf., A*, 2008, **319**, 165–172.

267 Lalhmunsima, R. R. Pawar, S.-M. Hong, K. J. Jin and S.-M. Lee, *J. Mol. Liq.*, 2017, **240**, 497–503.

268 N. Fatin-Rouge, A. Dupont, A. Vidonne, J. Dejeu, P. Fievet and A. Foissy, *Water Res.*, 2006, **40**, 1303–1309.

269 K. Yu, J. Ho, E. McCandlish, B. Buckley, R. Patel, Z. Li and N. C. Shapley, *Colloids Surf., A*, 2013, **425**, 31–41.

270 Y. Vijaya, S. R. Popuri, V. M. Boddu and A. Krishnaiah, *Carbohydr. Polym.*, 2008, **72**, 261–271.

271 P. Singh, S. K. Singh, J. Bajpai, A. K. Bajpai and R. B. Shrivastava, *J. Mater. Res. Technol.*, 2014, **3**, 195–202.

272 Y. Yan, Q. An, Z. Xiao, W. Zheng and S. Zhai, *Chem. Eng. J.*, 2017, **313**, 475–486.

273 M. Wang, X. Li, T. Zhang, L. Deng, P. Li, X. Wang and B. S. Hsiao, *Colloids Surf., A*, 2018, **558**, 228–241.

274 A. Sinha, B. G. Cha and J. Kim, *ACS Appl. Nano Mater.*, 2018, **1**, 1940–1948.

275 J. He, A. Cui, F. Ni, S. Deng, F. Shen and G. Yang, *J. Colloid Interface Sci.*, 2018, **531**, 37–46.

276 J. He, F. Ni, A. Cui, X. Chen, S. Deng, F. Shen, C. Huang, G. Yang, C. Song, J. Zhang, D. Tian, L. Long, Y. Zhu and L. Luo, *Sci. Total Environ.*, 2020, **701**, 134363.

277 A. Kumar, P. Paul and S. K. Nataraj, *ACS Sustainable Chem. Eng.*, 2017, **5**, 895–903.

278 Y. Li, H. Zhang, M. Fan, J. Zhuang and L. Chen, *Phys. Chem. Chem. Phys.*, 2016, **18**, 25394–25400.

279 J. Dai, Q. Tian, Q. Sun, W. Wei, J. Zhuang, M. Liu, Z. Cao, W. Xie and M. Fan, *Composites, Part B*, 2019, **160**, 480–487.

280 Y. Li, H. Zhang, C. Ma, H. Yin, L. Gong, Y. Duh and R. Feng, *Carbohydr. Polym.*, 2019, **226**, 115279.

281 J. Zhuang, J. Dai, S. H. Ghaffar, Y. Yu, Q. Tian and M. Fan, *Surf. Coat. Technol.*, 2020, **388**, 125551.

282 F. S. Mostafavi and D. Zaeim, *Int. J. Biol. Macromol.*, 2020, **159**, 1165–1176.

283 W. Y. Seow and C. A. E. Hauser, *J. Environ. Chem. Eng.*, 2016, **4**, 1714–1721.

284 N. A. Alygizakis, J. Urík, V. G. Beretsou, I. Kampouris, A. Galani, M. Oswaldova, T. Berendonk, P. Oswald, N. S. Thomaidis, J. Slobodnik, B. Vrana and D. Fatta-Kassinos, *Environ. Int.*, 2020, **138**, 105597.

285 M. M. Areco, S. Hanela, J. Duran and M. dos Santos Afonso, *J. Hazard. Mater.*, 2012, **213–214**, 123–132.

286 N. Gogoi, M. Barooah, G. Majumdar and D. Chowdhury, *ACS Appl. Mater. Interfaces*, 2015, **7**, 3058–3067.

287 J. Li, Z. Guo, S. Zhang and X. Wang, *Chem. Eng. J.*, 2011, **172**, 892–897.

288 Q. Zhang, S. Dan and K. Du, *Ind. Eng. Chem. Res.*, 2017, **56**, 8705–8712.

289 F. Luo, Z. Chen, M. Megharaj and R. Naidu, *Chem. Eng. J.*, 2016, **294**, 290–297.

290 G. U. Rani, A. K. Konreddy and S. Mishra, *Int. J. Biol. Macromol.*, 2018, **117**, 902–910.

291 T. Tang, K. Goossens, S. J. Lu, D. Meng and C. W. Bielawski, *RSC Adv.*, 2020, **10**, 29287–29295.

292 C. Cheng, Y. Cai, G. Guan, L. Yeo and D. Wang, *Angew. Chem., Int. Ed.*, 2018, **57**, 11177–11181.

293 L. Chen, Y. Li, Q. Du, Z. Wang, Y. Xia, E. Yedinak, J. Lou and L. Ci, *Carbohydr. Polym.*, 2017, **155**, 345–353.

294 P.-J. Lin, M.-C. Yang, Y.-L. Li and J.-H. Chen, *J. Membr. Sci.*, 2015, **475**, 511–520.

295 Z. Sun, J. Wang, Q. Wu, Z. Wang, Z. Wang, J. Sun and C.-J. Liu, *Adv. Funct. Mater.*, 2019, **29**, 1901312.

296 O. Duman, T. G. Polat, C. Diker and S. Tunç, *Int. J. Biol. Macromol.*, 2020, **160**, 823–835.

297 M. S. J. Khan, S. B. Khan, T. Kamal and A. M. Asiri, *Polym. Test.*, 2019, **78**, 105983.

298 B. N. Hoang, T. T. Nguyen, Q. P. T. Bui, L. G. Bach, D.-V. N. Vo, C. D. Trinh, X.-T. Bui and T. D. Nguyen, *J. Appl. Polym. Sci.*, 2020, **137**, 48904.

299 J. Shao, Z. Zhang, S. Zhao, S. Wang, Z. Guo, H. Xie and Y. Hu, *Starch*, 2019, **71**, 1800281.

300 M. Zhang, W. Jiang, D. Liu, J. Wang, Y. Liu, Y. Zhu and Y. Zhu, *Appl. Catal., B*, 2016, **183**, 263–268.

301 L. Tan, C. Yu, M. Wang, S. Zhang, J. Sun, S. Dong and J. Sun, *Appl. Surf. Sci.*, 2019, **467–468**, 286–292.

302 N. X. D. Mai, J. Bae, I. T. Kim, S. H. Park, G.-W. Lee, J. H. Kim, D. Lee, H. B. Son, Y.-C. Lee and J. Hur, *Environ. Sci. Nano*, 2017, **4**, 955–966.

303 M. Shorie, H. Kaur, G. Chadha, K. Singh and P. Sabherwal, *J. Hazard. Mater.*, 2019, **367**, 629–638.

304 W. Zhang, S. Shi, W. Zhu, L. Huang, C. Yang, S. Li, X. Liu, R. Wang, N. Hu, Y. Suo, Z. Li and J. Wang, *ACS Sustainable Chem. Eng.*, 2017, **5**, 9347–9354.

305 S. Patra, E. Roy, R. Madhuri and P. K. Sharma, *J. Ind. Eng. Chem.*, 2016, **33**, 226–238.

306 T. Brugnari, M. G. Pereira, G. A. Bubna, E. N. de Freitas, A. G. Contato, R. C. G. Corrêa, R. Castoldi, C. G. M. de Souza, M. Polizeli, A. Bracht and R. M. Peralta, *Sci. Total Environ.*, 2018, **634**, 1346–1351.

307 M. Dul, K. J. Paluch, H. Kelly, A. M. Healy, A. Sasse and L. Tajber, *Carbohydr. Polym.*, 2015, **123**, 339–349.

308 L. Li, R. Ni, Y. Shao and S. Mao, *Carbohydr. Polym.*, 2014, **103**, 1–11.

309 G. R. Mahdavinia, A. Massoudi, A. Baghban and B. Massoumi, *Iran. Polym. J.*, 2012, **21**, 609–619.

310 G. R. Mahdavinia and A. Asgari, *Polym. Bull.*, 2013, **70**, 2451–2470.

311 K. H. Kamala, S. Dacroryb, S. Alic, K. A. Alid and S. Kamelb, *Desalin. Water Treat.*, 2019, **165**, 281–289.

312 C. Liu, A. M. Omer and X. K. Ouyang, *Int. J. Biol. Macromol.*, 2018, **106**, 823–833.

313 M. Jabli, S. G. Almalki and H. Agougui, *Int. J. Biol. Macromol.*, 2020, **156**, 1091–1103.

314 M. Yang, X. Liu, Y. Qi, W. Sun and Y. Men, *J. Colloid Interface Sci.*, 2017, **506**, 669–677.

315 A. Prasannan, J. Udomsin, H.-C. Tsai, M. Sivakumar, C.-C. Hu, C.-F. Wang, W.-S. Hung and J.-Y. Lai, *J. Membr. Sci.*, 2020, **603**, 118026.

316 X. Liang, J. Duan, Q. Xu, X. Wei, A. Lu and L. Zhang, *Chem. Eng. J.*, 2017, **317**, 766–776.

317 H. Agougui, M. Jabli and H. Majdoub, *J. Appl. Polym. Sci.*, 2017, **134**, 45385.

318 F. H. H. Abdellatif and M. M. Abdellatif, *Cellulose*, 2020, **27**, 441–453.

319 A. Pourjavadi, M. Doulabi and M. Doroudian, *J. Iran. Chem. Soc.*, 2014, **11**, 1057–1065.

320 H. Mittal, A. Al Alili and S. M. Alhassan, *Cellulose*, 2020, **27**, 8269–8285.

321 S. Choudhury and S. K. Ray, *Carbohydr. Polym.*, 2018, **200**, 305–320.

322 A. A. Yakout, R. H. El-Sokkary, M. A. Shreadah and O. G. A. Hamid, *Carbohydr. Polym.*, 2016, **148**, 406–414.

323 L. Yang, N. Li, C. Guo, J. He, S. Wang, L. Qiao, F. Li, L. Yu, M. Wang and X. Xu, *Chem. Eng. J.*, 2021, **417**, 128051.

324 V. R. A. Ferreira, M. A. Azenha, C. M. Pereira and A. F. Silva, *J. Appl. Polym. Sci.*, 2020, **137**, 48842.

325 V. R. A. Ferreira, M. A. Azenha, C. M. Pereira and A. Fernando Silva, *Reactive and Functional Polymers*, 2017, **115**, 53–62.

326 V. R. A. Ferreira, M. A. Azenha, A. G. Bustamante, M. T. Mêna, C. Moura, C. M. Pereira and A. F. Silva, *Mater. Today Commun.*, 2016, **8**, 172–182.

327 C. Senthil and C. W. Lee, *Renewable Sustainable Energy Rev.*, 2021, **137**, 110464.

328 L. Peng, X. Duan, Y. Shang, B. Gao and X. Xu, *Appl. Catal., B*, 2021, **287**, 119963.

329 S. K. Bhatia, A. K. Palai, A. Kumar, R. K. Bhatia, A. K. Patel, V. K. Thakur and Y.-H. Yang, *Bioresour. Technol.*, 2021, **340**, 125644.

330 R. Gokulan, G. G. Prabhu, A. Avinash and J. Jegan, *Desalin. Water Treat.*, 2020, **184**, 340–353.

331 J. Wang, P. Nie, B. Ding, S. Dong, X. Hao, H. Dou and X. Zhang, *J. Mater. Chem. A*, 2017, **5**, 2411–2428.

332 M. Sharma, D. Mondal, N. Singh, K. Upadhyay, A. Rawat, R. V. Devkar, R. A. Sequeira and K. Prasad, *ACS Sustainable Chem. Eng.*, 2017, **5**, 3488–3498.

333 L. Hencz, X. Gu, X. Zhou, W. Martens and S. Zhang, *J. Mater. Sci.*, 2017, **52**, 12336–12347.

334 D. Li, G. Chang, L. Zong, P. Xue, Y. Wang, Y. Xia, C. Lai and D. Yang, *Energy Storage Mater.*, 2019, **17**, 22–30.

335 J. Nogueira, M. António, S. M. Mikhalev, S. Fateixa, T. Trindade and A. L. Daniel-da-Silva, *Nanomaterials*, 2018, **8**, 1004.

336 A. A. H. Saeed, N. Y. Harun, S. Sufian, A. A. Siyal, M. Zulfiqar, M. R. Bilad, A. Vagananthan, A. Al-Fakih,

A. A. S. Ghaleb and N. Almahbashi, *Sustainability*, 2020, **12**, 10318.

337 W. Deng, S. Tang, X. Zhou, Y. Liu, S. Liu and J. Luo, *Carbohydr. Polym.*, 2020, **247**, 116736.

338 K. Lu, Z. Min, J. Qin, P. Shi, J. Wu, J. Fan, Y. Min and Q. Xu, *Sci. Total Environ.*, 2021, **752**, 142282.

339 A. Mahto, A. Kumar, J. P. Chaudhary, M. Bhatt, A. K. Sharma, P. Paul, S. K. Nataraj and R. Meena, *J. Hazard. Mater.*, 2018, **353**, 190–203.

340 A. Mahto, A. Singh, K. Aruchamy, A. Maraddi, G. R. Bhadu, N. S. Kotrappanavar and R. Meena, *Sustainable Mater. Technol.*, 2021, **29**, e00292.

341 M. Zhu, A. Xia, Q. Feng, X. Wu, C. Zhang, D. Wu and H. Zhu, *Energy Technol.*, 2020, **8**, 1901215.

342 C. Chen, T. Ma, Y. Shang, B. Gao, B. Jin, H. Dan, Q. Li, Q. Yue, Y. Li, Y. Wang and X. Xu, *Appl. Catal., B*, 2019, **250**, 382–395.

343 Y.-m. Huang, G. Li, M. Li, J. Yin, N. Meng, D. Zhang, X.-q. Cao, F.-p. Zhu, M. Chen, L. Li and X.-j. Lyu, *Sci. Total Environ.*, 2021, **754**, 141999.

344 X.-y. Li, D. Han, J.-f. Xie, Z.-b. Wang, Z.-q. Gong and B. Li, *RSC Adv.*, 2018, **8**, 29237–29247.

345 L. Zhao, N. Baccile, S. Gross, Y. Zhang, W. Wei, Y. Sun, M. Antonietti and M.-M. Titirici, *Carbon*, 2010, **48**, 3778–3787.

346 A. Khan, M. Goepel, J. C. Colmenares and R. Gläser, *ACS Sustainable Chem. Eng.*, 2020, **8**, 4708–4727.

347 A. Khan, M. Goepel, J. C. Colmenares and R. Gläser, *ACS Sustainable Chem. Eng.*, 2020, **8**, 4708–4727.

348 M. Inagaki, M. Toyoda, Y. Soneda and T. Morishita, *Carbon*, 2018, **132**, 104–140.

349 M.-M. Titirici, R. J. White and L. Zhao, *Green*, 2012, **2**, 25–40.

350 A. Olejniczak, M. Lezanska, J. Włoch, A. Kucinska and J. P. Lukaszewicz, *J. Mater. Chem. A*, 2013, **1**, 8961–8967.

351 G. Daniel, Y. Zhang, S. Lanzalaco, F. Brombin, T. Kosmala, G. Granozzi, A. Wang, E. Brillas, I. Sirés and C. Durante, *ACS Sustainable Chem. Eng.*, 2020, **8**, 14425–14440.

352 Q. Liu, Y. Duan, Q. Zhao, F. Pan, B. Zhang and J. Zhang, *Langmuir*, 2014, **30**, 8238–8245.

353 L. Liu, Q.-F. Deng, X.-X. Hou and Z.-Y. Yuan, *J. Mater. Chem.*, 2012, **22**, 15540–15548.

354 W.-L. Zhang, Z.-B. Zhang, X.-H. Cao, R.-C. Ma and Y.-H. Liu, *J. Radioanal. Nucl. Chem.*, 2014, **301**, 197–205.

355 X. Zhong, Y. Sun, Z. Zhang, Y. Dai, Y. Wang, Y. Liu, R. Hua, X. Cao and Y. Liu, *J. Radioanal. Nucl. Chem.*, 2019, **322**, 901–911.

356 F. Shen, J. Su, X. Zhang, K. Zhang and X. Qi, *Int. J. Biol. Macromol.*, 2016, **91**, 443–449.

357 Q. Jin, Y. Li, D. Yang and J. Cui, *RSC Adv.*, 2018, **8**, 1255–1264.

358 Y. Liu, L. Li, Z. Duan, Q. You, G. Liao and D. Wang, *Colloids Surf., A*, 2021, **610**, 125728.

359 L. Zeng, X. Li, S. Fan, J. Mu, M. Qin, X. Wang, G. Gan, M. Tadé and S. Liu, *ACS Sustainable Chem. Eng.*, 2019, **7**, 5057–5064.

360 F. Marrakchi, M. J. Ahmed, W. A. Khanday, M. Asif and B. H. Hameed, *Int. J. Biol. Macromol.*, 2017, **98**, 233–239.

361 B. Chen, C. Zhang, L. Niu, X. Shi, H. Zhang, X. Lan and G. Bai, *Chem. – Eur. J.*, 2018, **24**, 3481–3487.

362 R. Gupta, N. Vadodariya, A. Mahto, J. P. Chaudhary, D. B. Parmar, D. N. Srivastava, S. K. Nataraj and R. Meena, *J. Appl. Electrochem.*, 2018, **48**, 37–48.

363 C. Chen, T. Ma, Y. Shang, B. Gao, B. Jin, H. Dan, Q. Li, Q. Yue, Y. Li and Y. Wang, *Appl. Catal., B*, 2019, **250**, 382–395.

364 E. Raymundo-Piñero, M. Cadek and F. Béguin, *Adv. Funct. Mater.*, 2009, **19**, 1032–1039.

365 S. Bo, X. Zhao, Q. An, J. Luo, Z. Xiao and S. Zhai, *RSC Adv.*, 2019, **9**, 5009–5024.

366 J. P. Chaudhary, A. Mahto, N. Vadodariya, F. Kholiya, S. Maiti, S. K. Nataraj and R. Meena, *RSC Adv.*, 2016, **6**, 61716–61724.

367 M. Yu, Y. Han, J. Li and L. Wang, *Int. J. Biol. Macromol.*, 2018, **115**, 185–193.

368 D. Nandan, G. Zoppellaro, I. Medřík, C. Aparicio, P. Kumar, M. Petr, O. Tomanec, M. B. Gawande, R. S. Varma and R. Zbořil, *Green Chem.*, 2018, **20**, 3542–3556.

369 S.-H. Ho, Y.-d. Chen, R. Li, C. Zhang, Y. Ge, G. Cao, M. Ma, X. Duan, S. Wang and N.-q. Ren, *Water Res.*, 2019, **159**, 77–86.

370 L. Shao, H. Liu, W. Zeng, C. Zhou, D. Li, L. Wang, Y. Lan, F. Xu and G. Liu, *Appl. Surf. Sci.*, 2019, **478**, 1017–1026.

371 X. Zhao, Q.-D. An, Z.-Y. Xiao, S.-R. Zhai and Z. Shi, *Chem. Eng. J.*, 2018, **353**, 746–759.

372 N. Farhadian, R. Akbarzadeh, M. Pirsheh, T. C. Jen, Y. Fakhri and A. Asadi, *Int. J. Biol. Macromol.*, 2019, **132**, 360–373.

373 K.-W. Jung and K.-H. Ahn, *Bioresour. Technol.*, 2016, **200**, 1029–1032.

374 S. Bo, X. Zhao, Q. An, J. Luo, Z. Xiao and S. Zhai, *RSC Adv.*, 2019, **9**, 5009–5024.

375 N. Alhokbany, T. Ahama, Ruksana, M. Naushad and S. M. Alshehri, *Composites, Part B*, 2019, **173**, 106950.

376 C. Lei, Y. Song, F. Meng, Y. Sun, D. C. W. Tsang, K. Yang and D. Lin, *Sci. Total Environ.*, 2021, **756**, 143866.

377 Y. Qi, B. Ge, Y. Zhang, B. Jiang, C. Wang, M. Akram and X. Xu, *J. Hazard. Mater.*, 2020, **399**, 123039.

378 Y. Wang, Q. Yang, J. Chen, J. Yang, Y. Zhang, Y. Chen, X. Li, W. Du, A. Liang, S.-H. Ho and J.-S. Chang, *J. Hazard. Mater.*, 2020, **395**, 122658.

379 B. Ghanim, T. F. O'Dwyer, J. J. Leahy, K. Willquist, R. Courtney, J. T. Pembroke and J. G. Murnane, *J. Environ. Chem. Eng.*, 2020, **8**, 104176.

380 X. Wang, C. Zhan, Y. Ding, B. Ding, Y. Xu, S. Liu and H. Dong, *ACS Sustainable Chem. Eng.*, 2017, **5**, 1457–1467.

381 L. Guo, Q.-D. An, Z.-Y. Xiao, S.-R. Zhai and L. Cui, *ACS Sustainable Chem. Eng.*, 2019, **7**, 9237–9248.

382 W. Zheng, Q. An, Z. Lei, Z. Xiao, S. Zhai and Q. Liu, *RSC Adv.*, 2016, **6**, 104897–104910.

383 X. Tian, H. Zhu, X. Meng, J. Wang, C. Zheng, Y. Xia and Z. Xiong, *ACS Sustainable Chem. Eng.*, 2020, **8**, 12755–12767.